



HAL
open science

Development of a detailed kinetic model for the combustion of biomass

Amal Dhahak, Roda Bounaceur, Céline Le Dreff-Lorimier, Guillaume Schmidt, Gwenaëlle Trouve, Frédérique Battin-Leclerc

► **To cite this version:**

Amal Dhahak, Roda Bounaceur, Céline Le Dreff-Lorimier, Guillaume Schmidt, Gwenaëlle Trouve, et al.. Development of a detailed kinetic model for the combustion of biomass. *Fuel*, 2019, 242, pp.756-774. 10.1016/j.fuel.2019.01.093 . hal-02390760

HAL Id: hal-02390760

<https://cstb.hal.science/hal-02390760>

Submitted on 3 Dec 2019

HAL is a multi-disciplinary open access archive for the deposit and dissemination of scientific research documents, whether they are published or not. The documents may come from teaching and research institutions in France or abroad, or from public or private research centers.

L'archive ouverte pluridisciplinaire **HAL**, est destinée au dépôt et à la diffusion de documents scientifiques de niveau recherche, publiés ou non, émanant des établissements d'enseignement et de recherche français ou étrangers, des laboratoires publics ou privés.

Development of a detailed kinetic model for the combustion of biomass

Amal Dhahak^a, Roda Bounaceur^a, Céline Le Dreff-Lorimier^b, Guillaume Schmidt^c,

Gwenaëlle Trouve^c, Frédérique Battin-Leclerc^{a,*}

^a Laboratoire Réactions et Génie des Procédés, CNRS, Université de Lorraine, Nancy, France

^b Centre Scientifique et Technique du Bâtiment, Nantes, France

^c Laboratoire Gestion des Risques et Environnement, Université de Haute-Alsace, Mulhouse, France

* Corresponding author: frederique.battin-leclerc@univ-lorraine.fr

ABSTRACT

In the context of the growing utilization of biomass to produce energy and of the related need to decrease pollutant emissions from domestic wood combustion devices, this paper presents a new kinetic model of wood combustion considering especially in details the gas-phase reactions related to the combustion of the tars produced by the biomass devolatilization. The tar production is predicted using a semi-detailed mechanism of the literature. The tar gas-phase combustion model has been built as a compilation of literature mechanisms already proposed for these species, except for hydroxyacetaldehyde for which a new oxidation mechanism has been written. Experiments on the thermochemical behavior of three types of wood (beech, fir and oak) were also performed in parallel of this work using Thermogravimetric Analysis (TGA). The new detailed kinetic model of wood combustion, BioPOx (Biomass Pyrolysis and Oxidation), has been tested against a wide range of experimental results published in literature. This model fairly reproduces experimental results for pyrolysis and combustion of biomass and its constituents, key produced tars from biomass pyrolysis, and key compounds for Polycyclic Aromatic Hydrocarbons (PAH) formation, for a wide range of experimental devices and operating conditions.

Keywords: Combustion; biomass; tars; detailed kinetic model; hydroxyacetaldehyde; Thermo-Gravimetric Analysis (TGA).

Introduction

The current global warming issues, especially the concerns about the alarming rise of atmospheric CO₂ [1], have increased the importance of the use of fuels from renewable resources, primarily biomass. The use of wood and biomass for domestic small combustion installations (fireplaces, stoves and boilers) is widely widespread in countries where heating is needed in winter [2]. Residential wood burning significantly affects the air quality because it is one of the largest sources of fine particles (PM_{2.5}, particulate matter of aerodynamic diameter below 2.5 μm). In addition, it is responsible for the emissions of a number of other pollutants (carbon and nitrogen monoxides, oxygenated hydrocarbons such as aldehydes and ketones, alcohols, furans and acids, PAH...)[3]. Environmentally sustainable wood heating will require a better understanding of the chemistry of the pollutant formation in such devices. Especially the development of kinetic models involving the chemical reactions responsible for pollutant formation is needed.

Lignocellulosic biomass pyrolysis and combustion are multi-scale, multi-phase, and multi-component processes [4], since biomass has a complex structure consisting mainly of a mixture of biopolymers: cellulose, hemicellulose, lignin with a small amount of extractives [5].

Biomass combustion includes four stages: drying, pyrolysis, homogeneous combustion of volatile products and heterogeneous combustion of char. Pyrolysis is the first step in any energy recovery processes such as combustion and gasification [6]. Modeling biomass pyrolysis is therefore essential for understanding combustion [7], which justifies the abundance of work in this field within the literature [8–11].

In the literature, two simplified approaches are generally proposed to describe biomass thermal degradation: the homogeneous approach, where biomass is considered as a homogeneous solid and the heterogeneous approach which takes into account the contribution of each biomass constituents (cellulose, hemicellulose and lignin) to the overall mechanism. According to the first approach, one or some global chemical reactions may be sufficient to describe wood devolatilization. A one-step global mechanism is the most simplified kinetic model used by many works in the literature [12–17]. Biomass decomposes into volatile compounds and a solid residue. This type of mechanism is generally used to model mass loss either by pyrolysis or thermogravimetric analysis (TGA) [8]. It is also used to model coupled chemical kinetics and physical phenomena, using for example a CFD (Computational Fluid Dynamics) approach [15][17]. The second common type of kinetic models in the homogeneous approach is independent competitive reaction scheme. According to this model, biomass produces competitively tar, gases, and char [2]. By using this reaction scheme, yields of tar, char and permanent gases can be predicted, which is not the case with one-step global mechanism. Generally, this second type of model is coupled to secondary reactions of tars formed during pyrolysis [18–22]. Multistep mechanisms are also discussed. In those schemes, an intermediate solid is formed by the first step and continues to decompose into secondary products [23].

According to the heterogeneous approach, the pyrolytic behavior of biomass is deduced from that of its major constituents: independent parallel reaction mechanisms, representing respectively cellulose, hemicellulose and lignin degradation, have been widely used to model biomass pyrolysis [24–26]. This type of mechanism allows a better prediction of product yields. It can be applied to a variety of biomass since the content of cellulose, hemicellulose and lignin differs from one type to another. Interactions between biomass constituents is neglected. A number of studies uses the Broido-Shafizadeh's scheme (Fig.1) to model biomass pyrolysis. This scheme, which was developed for the first time for cellulose degradation, has been applied

to lignin, hemicellulose and wood pyrolysis. Biomass is converted to intermediate solid called "active biomass" (reaction 1) which decomposes by competitive reactions (reactions 2 and 3) into gaseous, liquid and solid products [8].

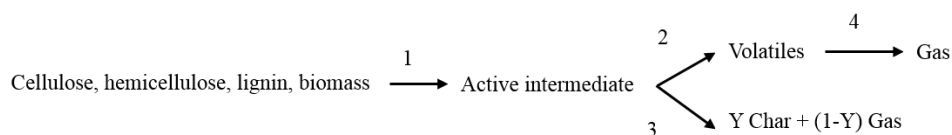


Fig.1. Broido-Shafizadeh's scheme to model biomass pyrolysis [27].

The most complex reaction scheme in the literature to simulate biomass pyrolysis following the heterogeneous approach is that of Ranzi who developed in 2008 a first multi-step semi-detailed mechanism [28] extending the Broido-Shafizadeh's approach. Dussan *et al.* proposed a new semi-detailed kinetic mechanism based on a recent Ranzi scheme [29] respectively for hemicellulose [30] and lignin pyrolysis [31]. More advanced approaches would involve micro-kinetic mechanistic models based on theoretical calculations as proposed by the Broadbelt team for cellulose [32–34] and hemicellulose [35] and by Horton *et al.* [36] for biomass pyrolysis and gasification.

Compared to pyrolysis, significantly fewer studies were published about the kinetic modelling of biomass combustion. Thermal degradation under oxidative atmosphere is indeed more complex. The presence of an oxidizing agent (air, oxygen, etc.) generates homogenous gas-phase reactions between oxygen and volatiles compounds released during devolatilization and heterogeneous reactions between oxygen and char [37].

A two-stage reaction kinetic scheme was proposed by Gil *et al.* [37] and Shen *et al.* [38] to represent biomass and char combustion. Pérez *et al.* [39] proposed a scheme including three independent reactions to represent respectively, cellulose, hemicellulose and lignin combustion coupled with a fourth reaction representing char oxidation. Wang *et al.* [40] consider two

simultaneous parallel reactions: an overall reaction describing biomass combustion and two individual reactions representing respectively volatiles and carbon residue oxidation. Navarrete Cereijo *et al.* [41] modeled biomass combustion as three sequential stages, which are drying, pyrolysis and char oxidation. In this work [41], as is shown in Fig.2, five reactions were used to represent biomass decomposition into tars (reaction 1) , volatiles (reaction 2) , and char (reaction 3), as well as tar degradation in volatiles (reaction 4) and char (reaction 5). The char combustion stage was modeled using three reactions (reactions 6, 7 and 8): direct combustion with oxygen and two reactions respectively with CO₂ and H₂O.

- (1) Biomass \rightarrow Tars
- (2) Biomass \rightarrow Volatiles
- (3) Biomass \rightarrow Char
- (4) Tars \rightarrow Volatiles
- (5) Tars \rightarrow Char
- (6) Char + O₂ \rightarrow CO₂
- (7) Char + CO₂ \rightarrow 2 CO
- (8) Char + H₂O \rightarrow CO + H₂

Fig.2. Kinetic scheme used by Navarrete Cereijo *et al.* to model biomass combustion [41].

A similar approach was used by Mätzing *et al.* [42] to model biomass combustion in fixed bed reactor with a slightly more detailed pyrolysis mechanism considering cellulose, hemicellulose and lignin devolatilization. However, approaches using global reactions cannot be an appropriate method to predict in details pollutant formation during biomass combustion in stoves or industrial systems for instance.

The main aim of this paper is to develop and validate a new detailed kinetic model of wood pyrolysis and combustion in order to predict pollutant emissions. This kinetic mechanism is tested against new TGA results obtained in parallel of this work, as well as a wide range of experimental results published in literature. The used literature results (29 datasets) and the

comparisons with the present model predictions have been collected and organized as a database given as two spreadsheets in Supplementary Material (SM).

I/ Description and validations of the chemical model

A new detailed kinetic mechanism, BioPOx, has been developed in Chemkin format. It includes two parts, (1) a semi-detailed mechanism to describe biomass pyrolysis, (2) a detailed mechanism of the gas-phase combustion of the volatiles species.

1.1. Semi-detailed mechanism to describe biomass pyrolysis and char combustion

1.1.a. Description of the model

From 2008, when the team of Ranzi [28] in Milano proposed the first multi-step semi-detailed mechanism to simulate biomass pyrolysis, this model has been progressively up-dated [29,43–46]. In this work, we used the 2016 version developed by Debiagi *et al.* [45] without change. This last kinetic mechanism consists of 27 semi-detailed reactions and 47 species. 22 species in the solid and metaplastic phase are involved. Thermodynamic data of these solid species are taken from [44]. The method for writing this mechanism is based on grouping similar species and lumping related reactions.

The model of Debiagi *et al.* [45] uses a detailed description of biomass, characterized as a mixture of three main constituents: cellulose, hemicellulose and lignin, the contents of which may significantly vary depending on the different types of biomass. Wood, even after drying, can still contains an average of 10-15% in mass of moisture [47]. However, since water can be considered mostly as a dilutant gas under the studied conditions, its amount has been neglected in this kinetic work. Hydrophobic and hydrophilic wood extractives, consisting mainly of terpenes, phenolic compounds, fatty and resin acids and triglycerides [48], were also neglected in our work as a first approach, because they account for less than 10% in mass of the entire biomass [28]. Lignocellulosic biomass is also characterized by a content of minerals

(potassium, calcium, sodium, silicon, phosphorus, chlorine and magnesium), less than 1% for wood [49]. In addition to the three main constituents, extractives and minerals, wood and woody biomass contains 0.1-0.7% of nitrogen and 0.01-0.42% of sulfur [47]. The presence of minerals, nitrogen and sulfur was not taken into account in our study.

Each constituent is represented by a pseudo-compound. Cellulose (CELL) is represented by the glucose monomer ($C_6H_{10}O_5$). Xylan ($C_5H_8O_4$) is the monomer chosen for hemicellulose (HCE). Lignin, having a complex structure, is represented by three reference compounds LIGC ($C_{15}H_{14}O_4$), LIGH ($C_{22}H_{28}O_9$), and LIGO ($C_{20}H_{22}O_{10}$), richer in C, H and O, respectively. The biomass characterization in this three constituents is a preliminary but a very important step. The characterization procedure consists of determining from the elemental composition of biomass (C/H/O, corrected by not considering water, N, S and other minerals), the biochemical composition in terms of cellulose, hemicellulose and lignin [29].

Assuming that there is no interaction between the three constituents, the devolatilization of biomass is thus considered a straightforward combination of the pyrolysis of the five reference components. As it will be described in part I.2, the produced volatile compounds may undergo secondary pyrolysis or combustion reactions in the gas phase. As shown in table 1, heterogeneous char combustion reactions were added to the model of Debiagi *et al.* [45] according to what was proposed by Navarrete Cereijo *et al.* [41] (see Fig. 2) and by Ranzi *et al.* [50].

Table 1: Heterogeneous char reactions (The rate constants [$k=AT^n \exp(-E_a/RT)$] are given in mol, s and cal units).

Reaction	A	n	Ea
(1) Char+O ₂ =>CO ₂	1.2e+10	0.0	32300.0
(2) Char+0.5O ₂ =>CO	2.5e+11	0.0	38200.0
(3) Char+H ₂ O=>CO ₂	2.5e+09	0.0	52000.0

I.1.b. Tests of the model

The model described in part I.1.a (in all this part, the model of Debiagi *et al.* [45] + the 3 reactions of Table 1 was used) has been tested both on TGA results obtained on purpose for this work, and on a wide range of literature results. The biomass characterization in this three constituents was taken from a database built in Milano [29].

I.1.b.α/ New TGA results

TGA experiments were carried out to study the thermal degradation of beech, oak and fir wood chips locally produced from the Alsacian forest and purchased from Agrivalor (Hirsingue, France). They were ground and sized to 4 mm of particle diameter. Hundred grams of each specie were dried at 105°C for 48h in an oven and then stored in a desiccator for further analyses. The physical and chemical properties of woods, as determined in the study of Schmidt *et al.* [51], are shown in table 2. TGA were performed from ground and dry wood samples (masses ranging from 5 to 10 mg) under an oxidative (air) atmosphere in a TA Instruments Q500 thermal analyzer under a temperature ramp equal to 5 °C.min⁻¹ from room temperature to 700°C. To confirm the reproducibility of results, the experiments were carried out at least six times, for each sample. The accuracy of the scale given by the manufacturer is about 0.1 µg. The standard deviations on the values of the maximum mass loss rates in DTG are from 1 to 2% whatever the nature of the sample. Since the model of Debiagi *et al.* [45] has been optimized for low heating rates, this new experimental study under oxidative conditions has been made with a heating rate lower to what can be found in literature.

Table 2: Physical and chemical properties of woods used in our TGA experiments according to Schmidt *et al.* [51].

Wood	Elemental (wt%)						Chemical (wt%)					Properties (%)	
	C	H	N	S	O	/	CELL	HCE	LIGC	LIGH	LIGO	Humidity ^a	Ash contents ^b
Fir	48,9	6,0	<0,1	<0,03	41,8	<3,3	45,0	24,4	4,0	21,1	5,5	24,6	0,36
Oak	48,5	5,9	<0,1	<0,03	42,7	<2,9	45,1	34,7	2,6	1,7	15,9	36,3	0,81
Beech	48,3	6,0	<0,1	<0,03	43,5	<2,2	53,5	25,1	0,0	5,8	5,8	41,4	1,40

a : On raw basis.

b: On dried basis.

/: Under-determined

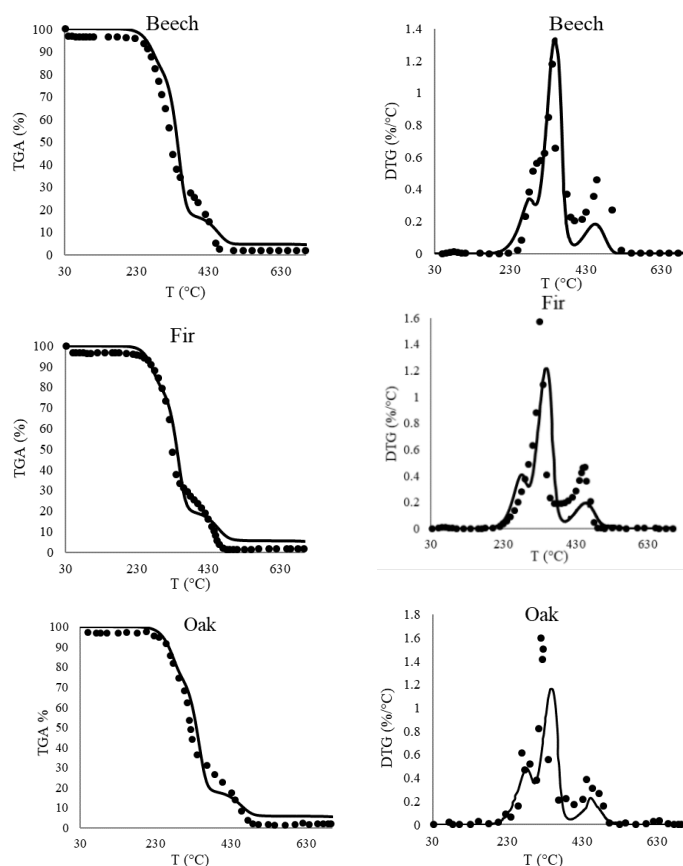


Fig.3. TGA and DTG (Derivative Thermo-Gravimetric) curves of beech, fir and oak wood under air at 5 °C/min (points: experimental data obtained in this work; lines: model predictions).

Thanks to the model previously described, the mass loss observed in these TGA experiments can be well predicted. Comparison between experimental results and model predictions of the thermal degradation of raw beech, fir and oak wood under air is shown in Fig.3. The small overprediction in TGA curves observed below 300°C is due to the fact that water evaporation

during the drying step is neglected. The agreement between experimental results and model predictions for TGA is better in case of fir which contains less amount of ashes than beech and oak, as shown in table 2. From DTG (Derivative Thermo-Gravimetric) curves, it is possible to obtain the instantaneous mass loss rates at all temperatures. Three steps can be distinguished as shown by the three peaks: the devolatilization of hemicellulose between 200 and 300°C, the devolatilization of cellulose, between 300 and 350°C, and the devolatilization of lignin accompanied by the char oxidation 400 and 500 °C.

1.1.b.β/ Tests against literature results

To better know the limitations of this model, we have tested it against the results of a wide range of experimental studies as shown in Table 3. These tests were performed on 10 cases of primary pyrolysis and TGA of wood or wood components (see details and results in a spreadsheet in supporting material).

The experimental studies 1, 2 and 6 were already modeled in the literature [28, 30, 31, 39, 41, 47] while the experimental studies 3-5 and 7-10 are simulated for the first time in this paper. As shown in Table 3, a majority of studies was performed using TGA. TGA experiments (as well as Derivative thermo-gravimetric (DTG) indicating mass loss rates) are modelled with the software CHEMKIN-PRO [53], considering the reactor as a Perfectly Stirred Reactor (PSR) or as a batch reactor if the sample is enclosed in a vessel.

Williams and Besler [54] studied the effect of the heating rate on the degradation of pine wood, cellulose and hemicellulose under an inert atmosphere (nitrogen). Two heating rates were used: 5 and 20° C.min⁻¹. Fig.4 compares model predictions and the experimental measurements of Williams and Besler [54] for degradation of pine wood and its constituents (cellulose and hemicellulose). The agreement between experimental results and model predictions is the best in the case of cellulose. The hemicellulose degradation, considered as a polymer of xylan,

begins at lower temperatures in experiments than what is predicted, because its decomposition forms more solid residue (20 wt%) than in the case of cellulose (5 to 10 wt%). Consequently, the predicted temperature for the start of the decomposition of the pine wood is also slightly higher than what was experimentally observed.

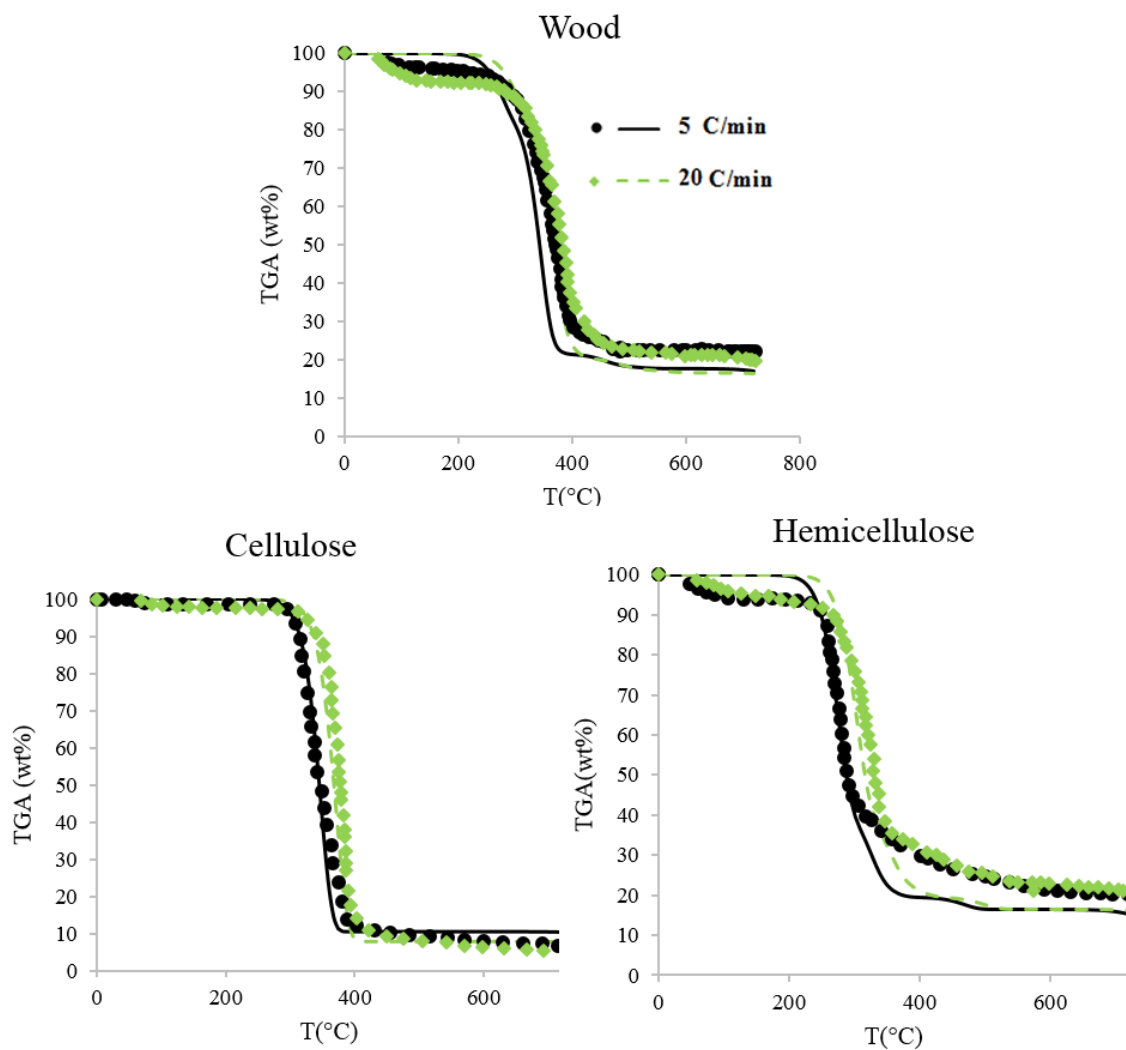


Fig.4. TGA curves of pine wood, cellulose and hemicellulose under nitrogen at 5 °C/min and 20 °C/min (points: experimental data [54]; lines: model predictions).

Table 3: Operating conditions considered for the tests of the model against experimental studies of devolatilization in the literature – Simulations for the studies in bold are shown in the text, simulations for the other studies are shown in SM. F : Simulated for the first time.

N°	Experimental study	Reactor	Studied compound	Dilutant	Temperature (°C)	Heating rate (°C/min)	Previous simulations
1	Jakab <i>et al.</i> 1995 [55]	TGA	6 types of lignin	Ar	200-900	20	[28,31,46,52]
2	Williams and Besler 1996 [54]	TGA	Pine wood, cellulose and hemicellulose	N ₂	300-720	5, 20, 40 and 80	[28,44,46,52]
3	Shen <i>et al.</i> 2009 [38]	TGA	Pine, aspen, birch and oak wood	Air	40-800	10 and 100	F
4	Shen <i>et al.</i> 2013 [56]	TGA	Lignin	He, He + 7%, 20%, 60% O ₂	20-800	20	F
5	Shen <i>et al.</i> 2013 [57]	TGA	Cellulose	He, He + 7%, 20%, 60% O ₂	50-800	20	F
6	Werner <i>et al.</i> 2014 [58]	TGA (DTG)	Cellulose, Xylan	N ₂	Final T = 600	10	[30]
7	Shen <i>et al.</i> 2015 [59]	TGA	Hemicellulose	He, He + 7%, 20%, 60% O ₂	20-800	20	F
8	Le Brech <i>et al.</i> 2016 [60]	U-shape fixed bed and TGA	Miscanthus, douglas, oak	Ar	20-Final T = 280, 300, 320, 350, 400 and 500	5	F
9	Le Brech <i>et al.</i> 2016 [61]		Miscanthus, and cellulose		Final T = 500		F
10	Chen <i>et al.</i> 2016 [62]	lab-scale fixed bed	Poplar wood	N ₂	400, 450, 500, 550 and 600	10, 30 and 50	F

In order to see the effect of adding air in TGA, Fig. 5 reports a comparison between predictions and experiments for oak thermal degradation respectively under air (this study, data of Fig. 3) and argon atmospheres by Le Brech *et al.* [60]. The difference between the two curves occurs mainly at high temperatures ($>400^{\circ}\text{C}$) where char reacts with oxygen from air.

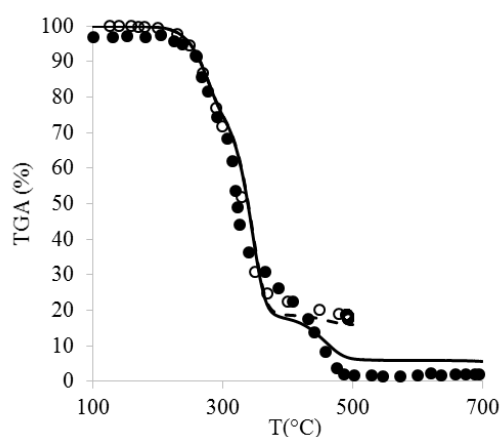


Fig.5. TGA curves of oak wood (full points: experimental data in air; empty points: experimental data in argon [60]; lines: model predictions (continuous line: in air, dashed line: in argon)).

The results shown here and in the spreadsheet of supplementary material show that, in most cases, for wood and its constituents, either under inert or oxidative atmosphere, the comparisons between TGA experiments and model predictions show reasonable agreement at low heating rates. The effect of a higher heating rate was studied by Shen *et al.* [38] using two types of wood: softwood (pine) and hardwood (birch, aspen and oak). Elemental, approximate and chemical compositions of the studied woods are shown in table 4. The thermal degradation of these biomasses under air, at two heating rates is shown in Fig.6. The model predictions of woods degradation at $10^{\circ}\text{C}/\text{min}$ are satisfactory while predicted TGA curves at $100^{\circ}\text{C}/\text{min}$ are slower than experiments. This is due to the fact that the model of Debiagi *et al.* [45] has been optimized for lower heating rates. Note however that the agreement is slightly better in the case

of pine and oak than for Aspens and birch containing more ashes, the possible catalytic effect of which is neglected in the model.

Table 4: Elemental, approximate and chemical compositions of woods used in the study of Shen et al. [38].

Wood	Elemental (wt%)					Approximate (wt%)			Chemical (wt%)				
	C	H	N	O	S	Humidity	Volatiles	Ash	CELL	HCE	LIGC	LIGH	LIGO
Pine	41,89	4,5	0,22	40,19	/	12,9	71,49	0,3	0,446	0,347	0,032	0,022	0,154
Aspens	45,84	5,22	0,36	39,97	0,01	8,19	80,37	0,41	0,567	0,274	0,000	0,051	0,108
Birch	44,41	3,48	0,27	36,65	/	11,39	74,36	0,76	0,526	0,271	0,000	0,099	0,104
Oak	45,37	5,03	0,28	41,29	0,01	8,78	76,82	0,24	0,451	0,347	0,026	0,017	0,159

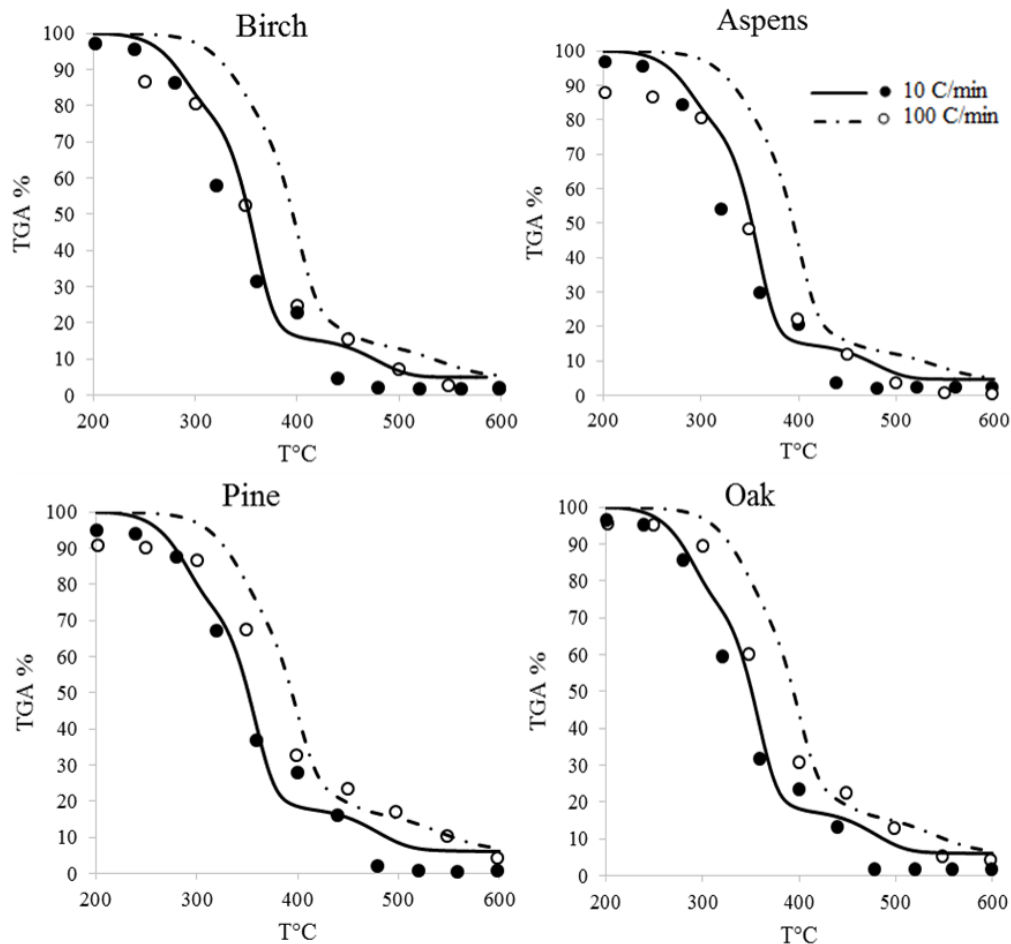


Fig.6. TGA curves of birch, aspen, pine and oak wood for two heating rates (points: experimental data [38]; lines: model predictions).

Kinetic mechanisms can also be used to predict product yields obtained during wood pyrolysis. One of the most detailed study of product yields during wood pyrolysis is that performed by Le Brech *et al.* [60] in a U-shape fixed bed reactor using two types of wood: oak and Douglas. The reactor was modelled as a Plug Flow Reactor (PFR). Fig. 7a reports the comparison between predictions and experiments for the mass loss during slow pyrolysis [60] and shows a satisfactory agreement.

Tar, solid and gas yields are shown in Fig. 7b, with an acceptable agreement between experiments and modeling.

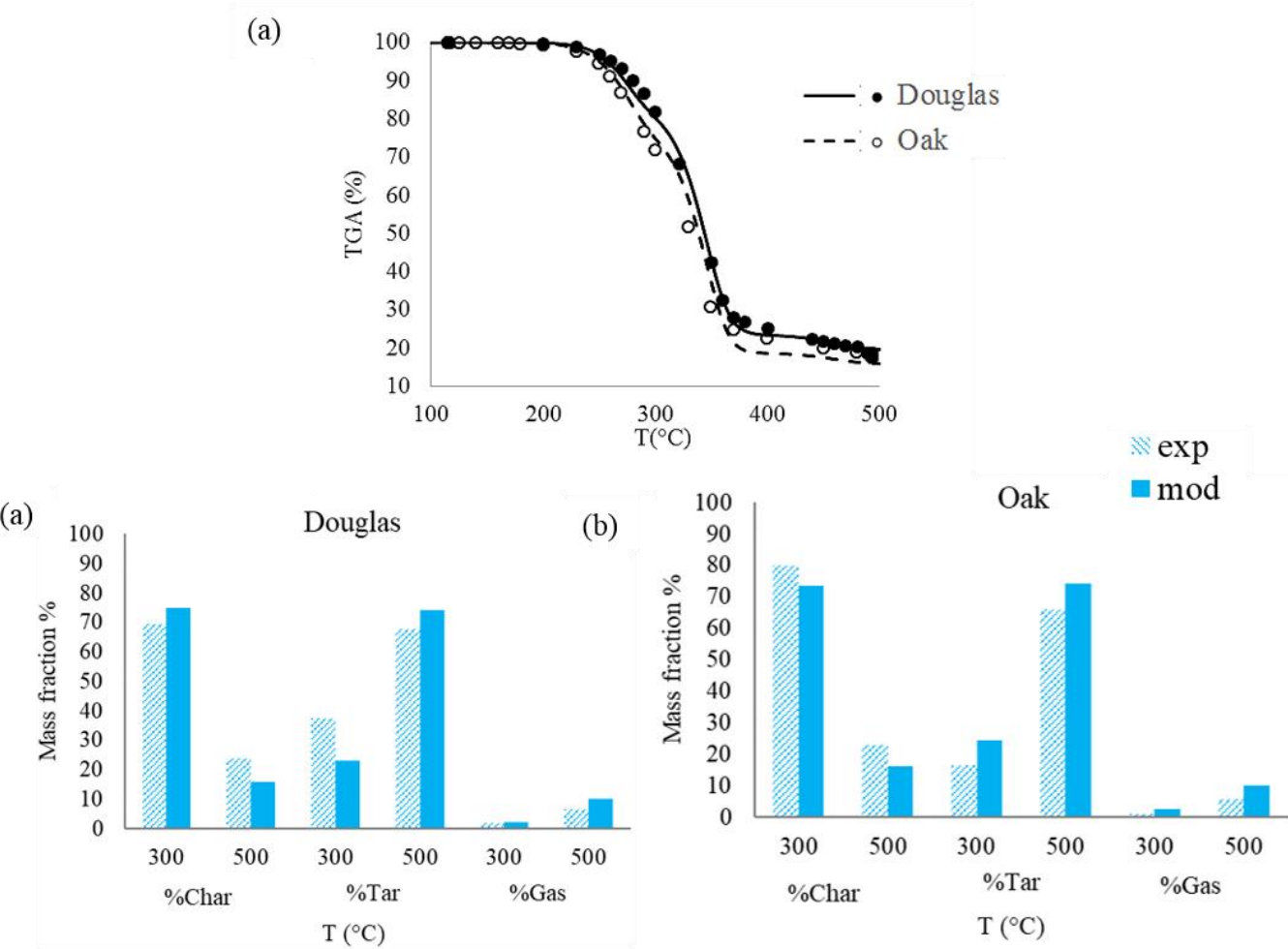


Fig.7. Slow pyrolysis of Douglas and oak wood as a function of temperature: (a) mass loss; (b) tar, solid and gas yields from the slow pyrolysis of Douglas and oak (shaded boxes: experimental data [60]; full boxes: model predictions).

For the same study [60], Fig.8 compares the predicted evolution of CO and CO₂, the main gaseous products, to experimental results [60]. In both model and experiments, CO₂ is the major gas compounds. The model predictions overestimate the mass fraction of CO₂ and CO for all the studied cases, except for CO mole fraction for oak pyrolysis at 300°C and for CO₂ mole fraction for oak pyrolysis at 500°C.

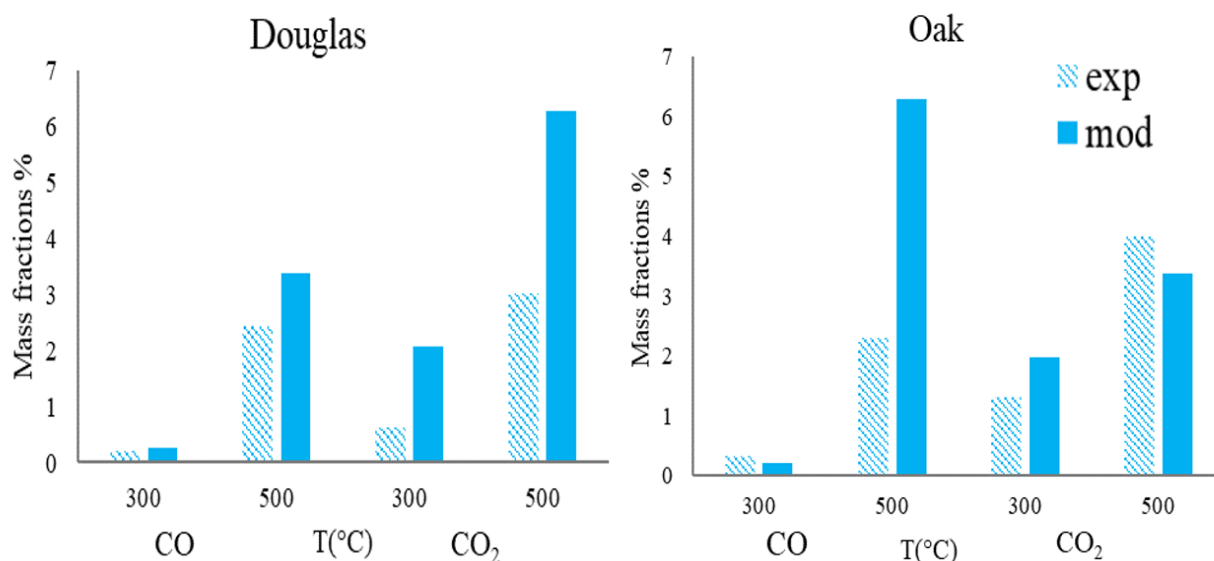


Fig.8. Slow pyrolysis of Douglas and oak wood as a function of temperature: CO and CO₂ yields (shaded boxes: experimental data [60]; full boxes: model predictions).

Using the same experimental set-up, Le Brech *et al.* [60] have also performed a study of Miscanthus pyrolysis (the experimental and simulated data for mass loss and tar, solid and gas (considered as the sum of CO, CO₂, H₂, CH₄, C₂H₄, C₂H₆ and C₆H₆) yields are given in SM). In this study, as is shown in Fig.9, the authors have also analyzed product yields for products gaseous at room temperature (CO₂ (Fig. 9a), CO (Fig. 9b) and CH₄ (Fig. 9c), as well as for one of the primary tars, phenol (Fig. 9d).

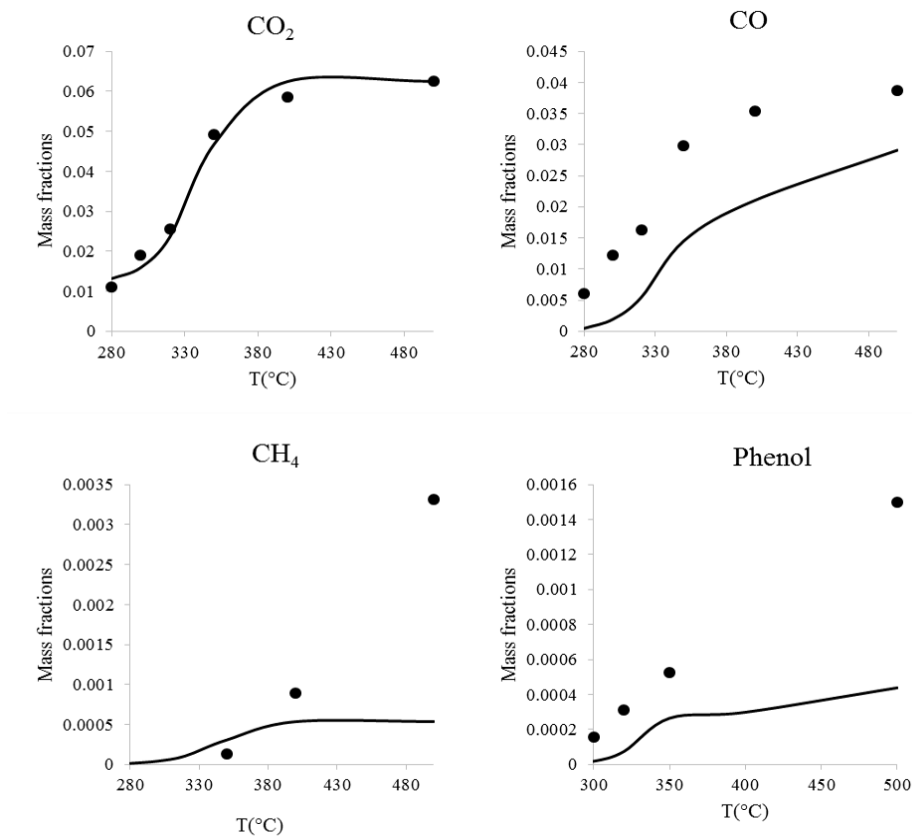


Fig.9. Slow pyrolysis of miscanthus: CO,CO₂ , CH₄ and phenol yields (points: experimental data [60]; lines: model predictions).

The model predictions of CO₂ formation during miscanthus pyrolysis are satisfactory while the mass fraction of CO and that of CH₄ are underestimated at high temperatures. The comparison between experimental and model predictions for phenol formation shows a reasonable agreement at low temperatures (< 400°C) for the shape of the temperature dependence.

In summary, thanks to this devolatilization model, for TGA under inert or oxidative atmosphere, the comparisons between experiments and model predictions show an acceptable agreement at low to moderate heating rates. Yields of primary pyrolysis products can also be fairly predicted until moderate temperatures. For high temperatures, gas-phase reactions effect cannot be neglected. Hence the need to consider primary tars degradation mechanism, which will be described in the next section.

1.2/ Detailed mechanism of the gas-phase combustion of the volatiles species

1.2.a. Description of the model

The second part of the BioPOx mechanism considers the gas-phase reactions induced by the combustion of the volatile species produced by the biomass devolatilization. As is shown in table 5, the BioPOx mechanism combines four chemical mechanisms: (1) a first one taken from [63] to describe the combustion of usual hydrocarbons, including aromatic compounds, such as benzene or toluene, or oxygenated compounds, such C₁-C₁₀ aldehydes or phenol, (2) a chemical mechanism for nitrogen oxides NO_x formation [64], (3) detailed mechanisms of the combustion of volatiles species chosen as surrogates of biomass tars, as shown in the table 6, and finally (4) the lumped mechanisms of the pyrolysis of levoglucosan (LVG), glyoxal and hydroxymethylfurfural (HMFU) taken from the secondary reactions proposed by Debiagi *et al.* [45]. All together, the BioPOx model (devolatilization + gas phase secondary pyrolysis and combustion) including 710 species and 5035 reactions, is given in Chemkin format in SM.

Table 5: Structure of BioPOx: detailed biomass combustion mechanism representing solid devolatilization, gas phase secondary pyrolysis and combustion.

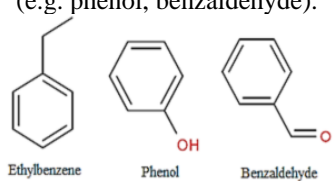
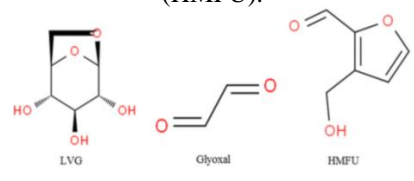
Hydrocarbon combustion	NO_x thermal formation	Combustion of key tar compound	Secondary pyrolysis of other volatile species
<i>Husson et al. 2013</i> [63]	<i>Song et al. 2018</i> [64]	<i>See Table 6</i>	<i>Debiagi et al. 2016</i> [45]
Detailed oxidation mechanisms of C ₀ -C ₈ hydrocarbons (e.g. ethylbenzene) and oxygenated compounds including aromatic ones (e.g. phenol, benzaldehyde).  Ethylbenzene Phenol Benzaldehyde	Detailed mechanism of NO _x formation.	Detailed mechanisms of the combustion of volatiles species chosen as surrogates of biomass tars	Semi-detailed mechanisms of the pyrolysis of levoglucosan (LVG), glyoxal and hydroxymethylfurfural (HMFU).  LVG Glyoxal HMFU

Table 6 reports the volatiles species chosen as surrogates of biomass tars. These compounds are produced from the primary pyrolysis of the three wood constituents. The mixture cellulose and

hemicellulose (holocellulose) is the source of hydroxyacetaldehyde, 5-methylfurfural, furfural and furan and its derivatives. Lignin can lead to the formation of anisole and guaiacol. Except for hydroxyacetaldehyde (HAA) for which a new oxidation mechanism has been written, the model used for the different listed surrogates are taken from literature as is shown in Table 7.

The most detailed models in the literature for LVG, HMFU and glyoxal decomposition are those already included in the lumped model of Debiagi *et al.* [45] which contains 3 types of metathesis and 5 unimolecular reactions for LVG, 1 type of metathesis and 2 unimolecular reactions for HMFU and 1 type of metathesis and 1 unimolecular reactions for glyoxal.

Table 6: Volatiles species chosen as surrogates of biomass tars.

Species (name in mechanism)	Chemical name	Formula	Structure	Mechanism
HOCHO	Formic acid	CH ₂ O ₂		Battin-Leclerc <i>et al.</i> 2008 [65]
CH ₃ CO ₂ H	Acetic acid	C ₂ H ₄ O ₂		Battin-Leclerc <i>et al.</i> 2008 [65]
C ₂ H ₄ O ₂	Hydroxyacetaldehyde (HAA)	C ₂ H ₄ O ₂		This study
Furan	Furan	C ₄ H ₄ O		Tran <i>et al.</i> 2017 [66]
MF	2-methylfuran	C ₅ H ₆ O		Tran <i>et al.</i> 2017 [66]
DMF	2,5-dimethylfuran	C ₆ H ₈ O		Tran <i>et al.</i> 2017 [66]
furylCHO	Furfural	C ₅ H ₄ O ₂		Nowakowska 2014 [67]
C ₆ H ₅ OCH ₃	Anisole	C ₇ H ₈ O		Nowakowska <i>et al.</i> 2014 [68]
MF-CHO	5-methylfurfural	C ₆ H ₆ O ₂		Nowakowska 2014 [67]
guaiacol	Guaiacol	C ₇ H ₈ O ₂		Nowakowska 2014 [67] [69]

Because HAA is one of the most important products derived from the pyrolysis of holocellulose and no more detailed model than that of Debiagi *et al.* [45] was available, we have developed a new dedicated mechanism. The new detailed kinetic mechanism for the pyrolysis and

oxidation of HAA is composed of 29 reactions, including unimolecular initiations, metathesis, decomposition and isomerization as is shown in table 7.

Vinyloxy and hydroxyl radicals are formed by breaking the HO-C bond (reaction 1 in table 7) while the breaking of C-C bond (reaction 2) leads to formyl radical (CHO) and CH₂OH radical. Hydroxyl-vinyloxy radical (R100HOCHCHO) and H-atom are obtained by breaking the OC-H bond (reaction 3). Reactions (4) and (5) produce R101OCH₂CHO and R102HOCH₂CO radicals by breaking respectively the H-OCCH and the HOCC-H bonds. Radicals R100HOCHCHO, R101OCH₂CHO and R102HOCH₂CO are also yielded by metathesis reactions (reactions 6-16). Metathesis reactions involved H-atom, hydroxyl, methyl, formyl and CH₂OH radicals. Radicals R100HOCHCHO and R101OCH₂CHO can interchange by isomerization by internal H-transfer (17) and lead to radical R102HOCHO (reactions 18 and 19). R103HOC₂H₄O and R104HOCHCHOH are obtained by H-addition on the C=O bond (reactions 20 and 21).

R100HOCHCHOH can react by breaking a C-H bond yielding glyoxal (reaction 22).

R101OCH₂CHO can react by β -scissions by breaking a C-C bond to give formaldehyde and CHO radical (reaction 23) and by breaking a C-H bond yielding glyoxal (reaction 24).

R102HOCHO can react by α -scissions to produce CO and CH₂OH radical (reaction 25), which can easily isomerize in formaldehyde, by β -scissions by breaking a C-O bond to give ketene and OH radical (reaction 26), and by β -scissions by breaking a C-H bond yielding glyoxal (reaction 27).

R103HOC₂H₄O can react by β -scissions by breaking a C-C bond to give formaldehyde and CH₂OH radical (reaction 28).

R104HOCHCHOH can react by β -scissions by breaking a C-C bond to form acetaldehyde and OH radical (reaction 29).

Thermodynamic data were calculated based on group additivity Benson method using THERGAS software [70]. Kinetic rate constants were determined by analogy with those of similar reactions (see footnotes in Table 7).

Table 7: Primary mechanism for HAA oxidation. The rate constants ($k=AT^n\exp(Ea/RT)$) are given in mol, s and cal units).

Reaction	A	n	Ea	References
Unimolecular initiation				
(1) $\text{OH}+\text{CH}_2\text{CHO}=\text{C}_2\text{H}_4\text{O}_2$	6.0e+13	0.0	0.0	Estimated ^a
(2) $\text{C}_2\text{H}_4\text{O}_2 = \text{CHO}+\text{CH}_2\text{OH}$	6.0e+14	0.0	79100.0	Estimated ^b
(3) $\text{H}+\text{R100HOCHCHO} =\text{C}_2\text{H}_4\text{O}_2$	1.0e+14	0.0	0.0	Estimated ^c
(4) $\text{H}+\text{R101OCH}_2\text{CHO} =\text{C}_2\text{H}_4\text{O}_2$	1.0e+14	0.0	0.0	Estimated ^c
(5) $\text{H}+\text{R102HOCH}_2\text{CO} =\text{C}_2\text{H}_4\text{O}_2$	1.0e+14	0.0	0.0	Estimated ^c
Metathesis				
(6) $\text{C}_2\text{H}_4\text{O}_2+\text{H} = \text{R100HOCHCHO}+\text{H}_2$	3.0e+14	0.0	10000.0	Estimated ^d
(7) $\text{C}_2\text{H}_4\text{O}_2+\text{H} = \text{R101OCH}_2\text{CHO}+\text{H}_2$	4.2e+06	2.1	4900.0	Estimated ^e
(8) $\text{C}_2\text{H}_4\text{O}_2+\text{H} = \text{R102HOCH}_2\text{CO}+\text{H}_2$	4.0e+13	0.0	4200.0	Estimated ^e
(9) $\text{C}_2\text{H}_4\text{O}_2+\text{OH} = \text{R100HOCHCHO}+\text{H}_2\text{O}$	1.0e+13	0.0	2000.0	Estimated ^d
(10) $\text{C}_2\text{H}_4\text{O}_2+\text{OH} = \text{R101OCH}_2\text{CHO}+\text{H}_2\text{O}$	5.4e+05	2.0	-340.0	Estimated ^e
(11) $\text{C}_2\text{H}_4\text{O}_2+\text{OH} = \text{R102HOCH}_2\text{CO}+\text{H}_2\text{O}$	4.2e+12	0.0	5000.0	Estimated ^e
(12) $\text{C}_2\text{H}_4\text{O}_2 +\text{CH}_3 = \text{R100HOCHCHO}+\text{CH}_4$	4.0e+12	0.0	11000.0	Estimated ^d
(13) $\text{C}_2\text{H}_4\text{O}_2+\text{CH}_3 = \text{R101OCH}_2\text{CHO}+\text{CH}_4$	6.7e+08	3.1	6935.0	Estimated ^e
(14) $\text{C}_2\text{H}_4\text{O}_2+\text{CH}_3 = \text{R102HOCH}_2\text{CO}+\text{CH}_4$	2.0e-06	5.6	2500.0	Estimated ^e
(15) $\text{C}_2\text{H}_4\text{O}_2+\text{CHO} = \text{R102HOCH}_2\text{CO}+\text{HCHO}$	2.0e-06	5.6	2500.0	Estimated ^e
(16) $\text{C}_2\text{H}_4\text{O}_2+\text{CH}_2\text{OH} = \text{R102HOCH}_2\text{CO}+\text{CH}_3\text{OH}$	2.0e-06	5.6	2500.0	Estimated ^e
Isomerization				
(17) $\text{R101OCH}_2\text{CHO} = \text{R100HOCHCHO}$	6.5e+11	1.0	33400.0	Estimated ^f
(18) $\text{R100HOCHCHO} = \text{R102HOCH}_2\text{CO}$	3.2e+11	1.0	30100.0	Estimated ^f
(19) $\text{R101OCH}_2\text{CHO} = \text{R102HOCH}_2\text{CO}$	1.9e+12	1.0	27600.0	Estimated ^f
Additions				
(20) $\text{R103HOC}_2\text{H}_4\text{O} = \text{C}_2\text{H}_4\text{O}_2+\text{H}$	2.0e+14	0.0	23300.0	Estimated ^g
(21) $\text{R104HOCH}_2\text{CHOH} = \text{C}_2\text{H}_4\text{O}_2+\text{H}$	3.0e+13	0.0	38000.0	Estimated ^g
Reactions of R100HOCHCHO				
(22) $\text{R100HOCHCHO} = \text{CHOCHO}+\text{H}$	3.0e+13	0.0	34800.0	Estimated ^h
Reactions of R101OCH2CHO				
(23) $\text{R101OCH}_2\text{CHO} = \text{HCHO}+\text{CHO}$	8.0e+13	0.0	21500.0	Estimated ^d
(24) $\text{R101OCH}_2\text{CHO} = \text{CHOCHO}+\text{H}$	2.0e+14	0.0	23300.0	Estimated ^d
Reactions of R102HOCH2CO				
(25) $\text{CO}+\text{R6CH}_2\text{OH} = \text{R102HOCH}_2\text{CO}$	5.0e+11	0.0	6900.0	Estimated ^a
(26) $\text{CH}_2\text{CO}+\text{OH} = \text{R102HOCH}_2\text{CO}$	5.4e+12	0.0	00000.0	Estimated ^a
(27) $\text{CHOCHO}+\text{H} = \text{R102HOCH}_2\text{CO}$	7.5e+12	1.0	1450.0	Estimated ^d
Reactions of R103HOC2H4O				
(28) $\text{R103HOC}_2\text{H}_4\text{O} = \text{CH}_2\text{OH}+\text{HCHO}$	8.0e+13	0.0	21500.0	Estimated ^d
Reactions of R104HOCH2CHOH				
(29) $\text{R104HOCH}_2\text{CHOH} \Rightarrow \text{OH}+\text{CH}_3\text{CHO}$	6.1e+11	0.0	23600.0	Estimated ^g

a: Rate constant taken equal to that the recombination of methyl and hydroxyl radicals to form methanol as proposed by Baulch *et al.* [71]: $\text{CH}_3+\text{OH}=\text{CH}_3\text{OH}$.

b: Rate constant taken equal to that the unimolecular initiation of acetaldehyde as proposed by Yasunaga *et al.* [72] : with the A-factor multiplied by 0.4.

c: Rate constant taken equal to that of the recombination of H atoms with alkyl radicals as proposed by Allara et Shaw [73].

d: Analogy-Rate constant taken equal to that of the similar reaction in the case the pyrolysis of acetaldehyde proposed by Yasunaga *et al.* [72].

e: Analogy-Rate constant taken equal to that of the similar reaction in the case the pyrolysis or oxidation of methanol or acetaldehyde as proposed by Baulch *et al.* [71].

f: Rate calculated using software KINGAS [74].

g: Analogy-Rate constant taken equal to that of the similar reaction in the case the oxidation of ethanol as proposed by Tran *et al.* [75].

h: Analogy-Rate constant taken equal to that of the similar reaction in the case the oxidation of ethanol as proposed by Tran *et al.* [75]: $\text{C}_2\text{H}_4\text{OH}=\text{H}+\text{CH}_3\text{CHO}$.

I.2.b. Validation of the model

The BioPOx model has been validated on 19 gas-phase pyrolysis and combustion studies of key compounds of biomass pyrolysis (HAA, anisole, furan and its derivatives, furfural and 5-methylfurfural, guaiacol, phenol and levoglucosan (LVG)), of key compounds for PAH formation (benzene, ethylbenzene, toluene, acetylene ...) and of biomass and its constituents as shown in Table 8. The experimental studies 1, 3, 4-8, 10-13 and 15-19 were already modeled in the literature while the experimental studies 2, 9 and 14 are simulated for the first time in this paper. Fig.9 and Fig.10 display comparisons between model and experiments for two examples of key primary products from holocellulose. Fig.10 shows the comparison between BioPOx predictions and experimental results for the decomposition of HAA in an isothermal tubular reactor at different temperatures: 625, 650, 675 and 700 °C [76]. These experimental results, which are the only available ones for the decomposition of HAA, were already used as a validation target by Ranzi *et al.* [28] using their model. Thanks to the newly developed HAA mechanism, BioPOx model predictions are in better agreement with the experimental results than those of the model of Debiagi *et al.* [45], but it will still need refinements when new experimental data are available.

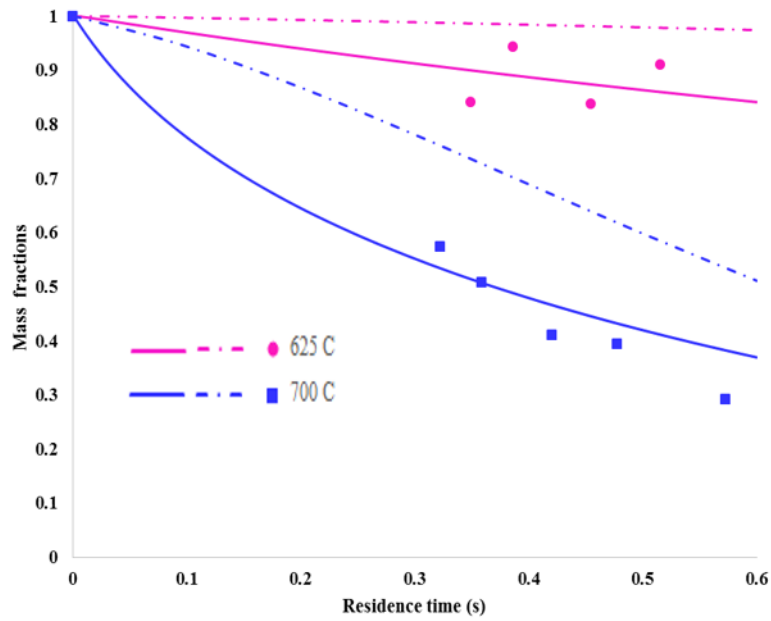


Fig.10. HAA pyrolysis at 625 and 700°C : Comparisons between model predictions (BioPOx model: continuous lines, Debiagi *et al.* [45] dashed lines) and experimental data (points) [76].

The second example of key products from holocellulose concerns LVG, the major product of cellulose pyrolysis. LVG pyrolysis was investigated by Fukutome *et al.* [77] in a tubular reactor at temperatures between 400 and 900 °C. Fig.11 reports the comparison between model prediction and experimental results which are in good agreement for LVG consumption and not so far for most of the observed products.

Table 8: Operating conditions of the tests of the model against experimental gas-phase pyrolysis and combustion studies. Simulations for the studies in bold are shown in the text, simulations for the other studies are shown in SM.

N ^o	Studied compound	Experimental study	Process	Reactor	Temperature (°C)	Pressure (kPa)	Residence time (sec)	Equivalence ratio	Previous simulations	Model*
Biomass and its constituents										
1	Cedar wood	Thimthong <i>et al.</i> 2015 [78]	Pyrolysis and partial oxidation of volatile compounds	Two-stage tubular	700 and 800	/	/	/	[78]	Yes
2	Pine wood	Hoekstra <i>et al.</i> 2011 [79]	Pyrolysis and secondary reactions of volatile compounds	Fluidized bed and tubular reactor in series	500	/	Fluidized bed 1.5 sec	/	F	No
3	Cellulose	Norinaga <i>et al.</i> 2013 [80]	Pyrolysis and secondary reactions of volatile compounds	Two-stage tubular	700,750 and 800	/	6	/	[80]	Yes
Key compounds of biomass combustion: holocellulose										
4	HAA	Shin <i>et al.</i> 2001 [76]	Pyrolysis	Tubular	625, 650, 675 and 700	/	/	/	[28],[45]	No
5	Furan, MF and DMF	Tran <i>et al.</i> 2017 [66]	Oxidation	Tubular	397-897	100	/	~ 0.5 ,1 and 2	[66]	Yes
6		Cheng <i>et al.</i> 2017 [81]	Pyrolysis	Tubular	827-1327	4	/	/	[81]	Yes
7	Furfural	Zhang <i>et al.</i> 2017 [82]	Pyrolysis	Tubular	100-1000	101.3	/	/	[82]	Yes
8	5-methylfurfural	Nowakowska <i>et al.</i> 2014 [67]	Pyrolysis	JSR	400-850	106.7	2	/	[67]	Yes
			Oxidation		400-725			0.8		Yes
9	LVG	Fukutome <i>et al.</i> 2015 [77]	Pyrolysis	Two-stage tubular	400-900	/	0.8-1.4	/	F	No

N°	Studied compound	Experimental study	Process	Reactor	Temperature (°C)	Pressure (kPa)	Residence time (sec)	Equivalence ratio	Previous simulations	Model*
Key compounds of biomass combustion: lignin										
10	Anisole	Nowakowska <i>et al.</i> 2014 [68]	Pyrolysis and oxidation	JSR	400-900	106.7	2	1	[68]	Yes
11		Zhang <i>et al.</i> 2017 [82]	Pyrolysis	Tubular	100-1000	101.3	/	/	[82]	Yes
12	Guaiacol	Zhang <i>et al.</i> 2017 [82]	Pyrolysis	Tubular	100-1000	101.3	/	/	[82]	Yes
13		Nowakowska <i>et al.</i> 2014 [67][69]	Pyrolysis	JSR	250-625	106.7	2	1	[67][69]	Yes
			Oxidation		300-650					Yes
14	Asmadi <i>et al.</i> 2011 [83]	Pyrolysis	Closed ampoule	400-600	/	40-600	/	F	No	
15	Phenol	Alzueta <i>et al.</i> 2000 [84]	Pyrolysis	Tubular	627-1177	/	165/T(K)	/	[84]	Yes
			Oxidation				115/T(K)			Yes
Key compounds for PAH formation										
16	Acetylene	Wang <i>et al.</i> 2017 [85]	Oxidation	JSR	327-827	101.3	/	0.5, 1, 2 and 3	[85]	Yes
17	Ethylbenzene	Yuan <i>et al.</i> 2016 [86]	Pyrolysis	Tubular	850-1500	4, 20 and 101.3	/	/	[86]	Yes
			Oxidation	Sphere	726-943, 726-1105 and 824-1125	/	0.12 and 0.15	0.5, 1 and 1.5		Yes
18	Benzene	Alzueta <i>et al.</i> 2000 [84]	Oxidation	Tubular	627-1177	/	178/T(K) or 187/T(K)	/	[84,87]	Yes
19	Toluene	Zhang <i>et al.</i> 2017 [82]	Pyrolysis	Tubular	100-1000	101.3	/	/	[82]	Yes

* Kinetic model developed together with the experimental study.

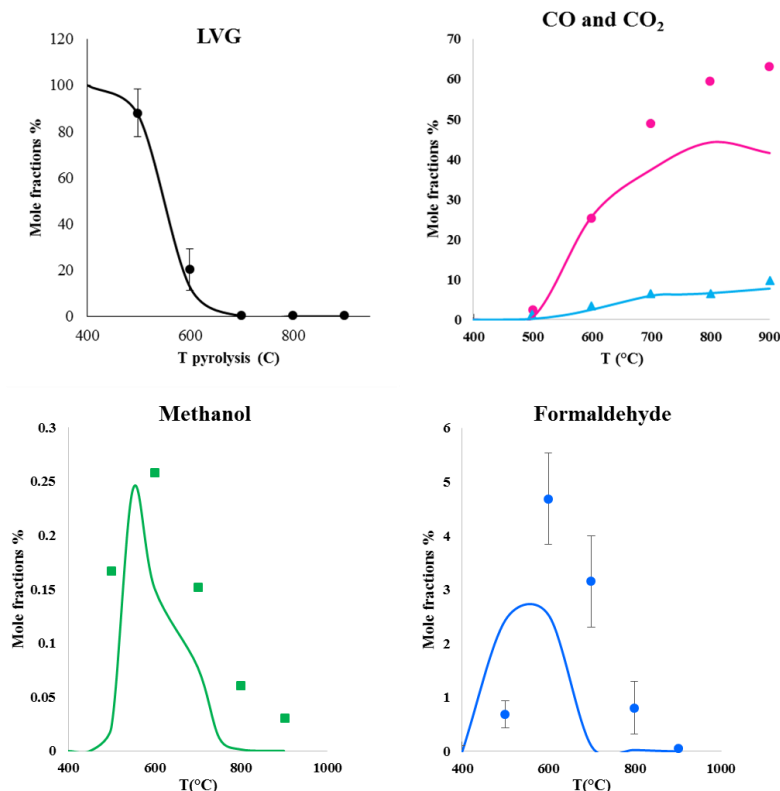


Fig.11. LVG pyrolysis: Comparisons between model predictions (lines) and experimental data [77], error bars are the standard deviations provided by the authors.

The results shown here and in the spreadsheet in supplementary material show that, in most of cases, for key products from holocellulose (furan and its derivatives, furfural), the comparisons between pyrolysis and/or oxidation experiments and BioPOx predictions show reasonable agreement.

Fig.12 presents simulations and experimental results of the pyrolysis and oxidation of anisole, also called methoxybenzene ($\text{CH}_3\text{OC}_6\text{H}_5$), which is representative of lignin tars. The decomposition of this molecule, under inert and oxidative atmospheres, was studied by Nowakowska *et al.* [68] in a Jet-Stirred Reactor (JSR). As shown in Fig.12, the agreement between experimental points and BioPOx predictions has not been deteriorated by adding the parts of the BioPOx model (devolatilization model, mechanisms of the combustion of other volatiles species (HAA, LVG, HMFU, guaiacol...), detailed mechanism of NO_x formation) that were not present in the original mechanism of Nowakowska *et al.* [68]. In contrast, a

slightly better agreement was found between experimental points and BioPOx predictions for some products, except for the formation of phenol during oxidation.

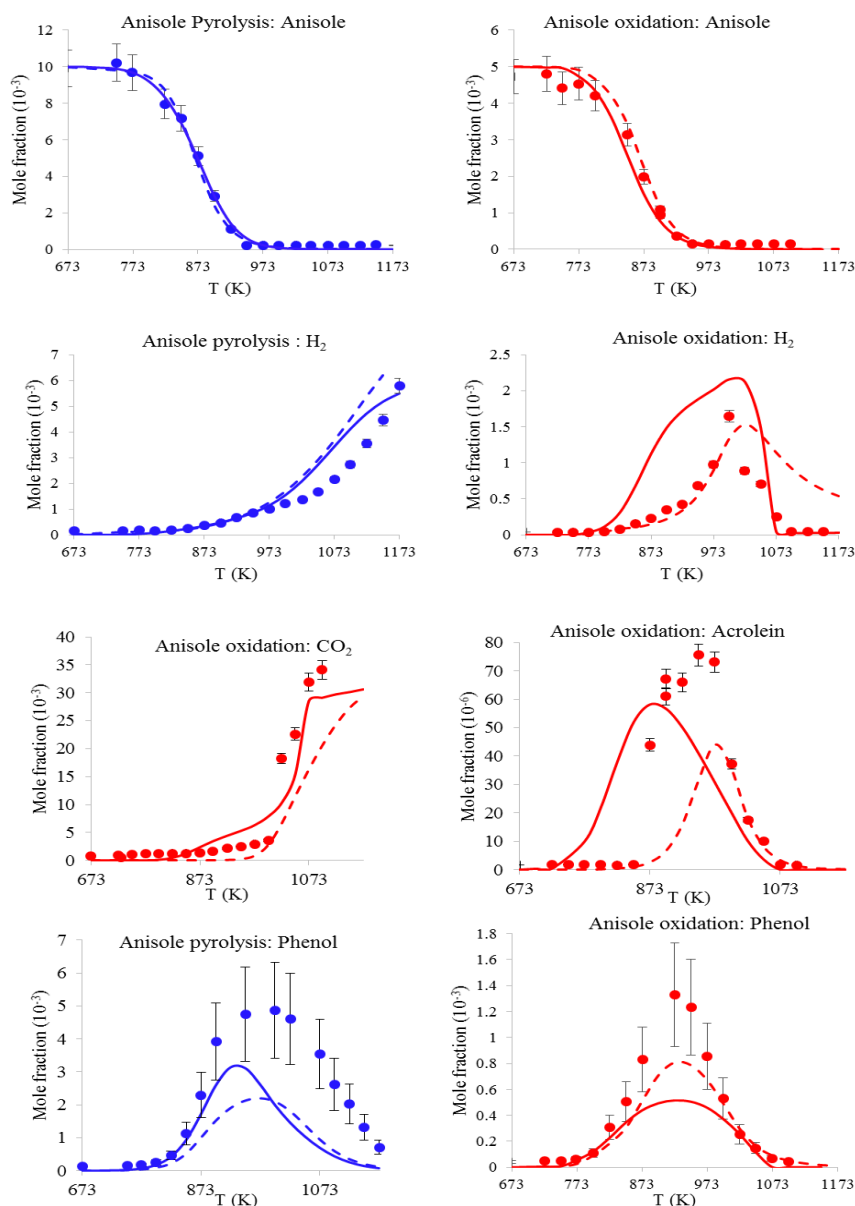


Fig.12. Anisole pyrolysis and oxidation: Comparisons between model predictions (BioPOx : continuous lines, Nowakoswka *et al.* [68]: dashed lines) and experimental data (points) [68], error bars are the uncertainties provided by the authors.

The difference between the predictions using both models can be partly explained by the presence of a guaiacol sub-mechanism in BioPOx, since guaiacol is an important product of the decomposition of anisole.

As shown in the spreadsheet of supplementary material, BioPOx can also fairly predict the conversion rate of anisole during pyrolysis conducted in a tubular reactor by Zhang *et al.* [82] at temperatures between 100 and 1000°C.

Guaiacol, also called 2-methoxyphenol, is another example of key products from the lignin. The pyrolysis and/or the oxidation of this species used as a surrogate for lignin primary tars, was studied by Nowakowska *et al.* [67], Zhang *et al.* [82] and Asmadi *et al.* [83]. Comparisons between experiments and BioPOx predictions, which are in good agreement, are shown in Fig. 13 and in the spreadsheet of supplementary material.

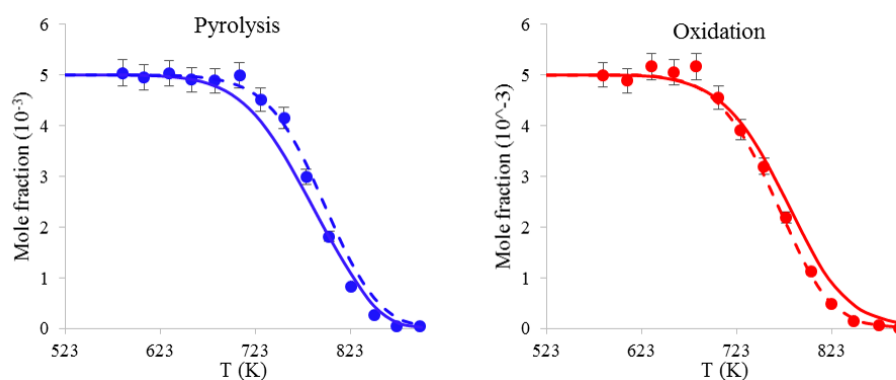


Fig.13. Guaiacol pyrolysis and oxidation: Comparisons between model predictions (BioPOx: continuous lines, Nowakowska *et al.* [68]: dashed lines) and experimental data (points) [67], error bars are the uncertainties provided by the authors.

The pyrolysis and combustion of key compounds for PAH formation has also been studied with the BioPOx model. Acetylene is the lightest and one of the most important key compounds for PAH formation. Fig.14 reports the comparison between model predictions and experimental results for acetylene consumption and ethylene production during acetylene oxidation studied in a JSR by Wang *et al.* [85]. The model predictions in lean and stoichiometric conditions are satisfactory while acetylene degradation in rich mixture is faster than predictions.

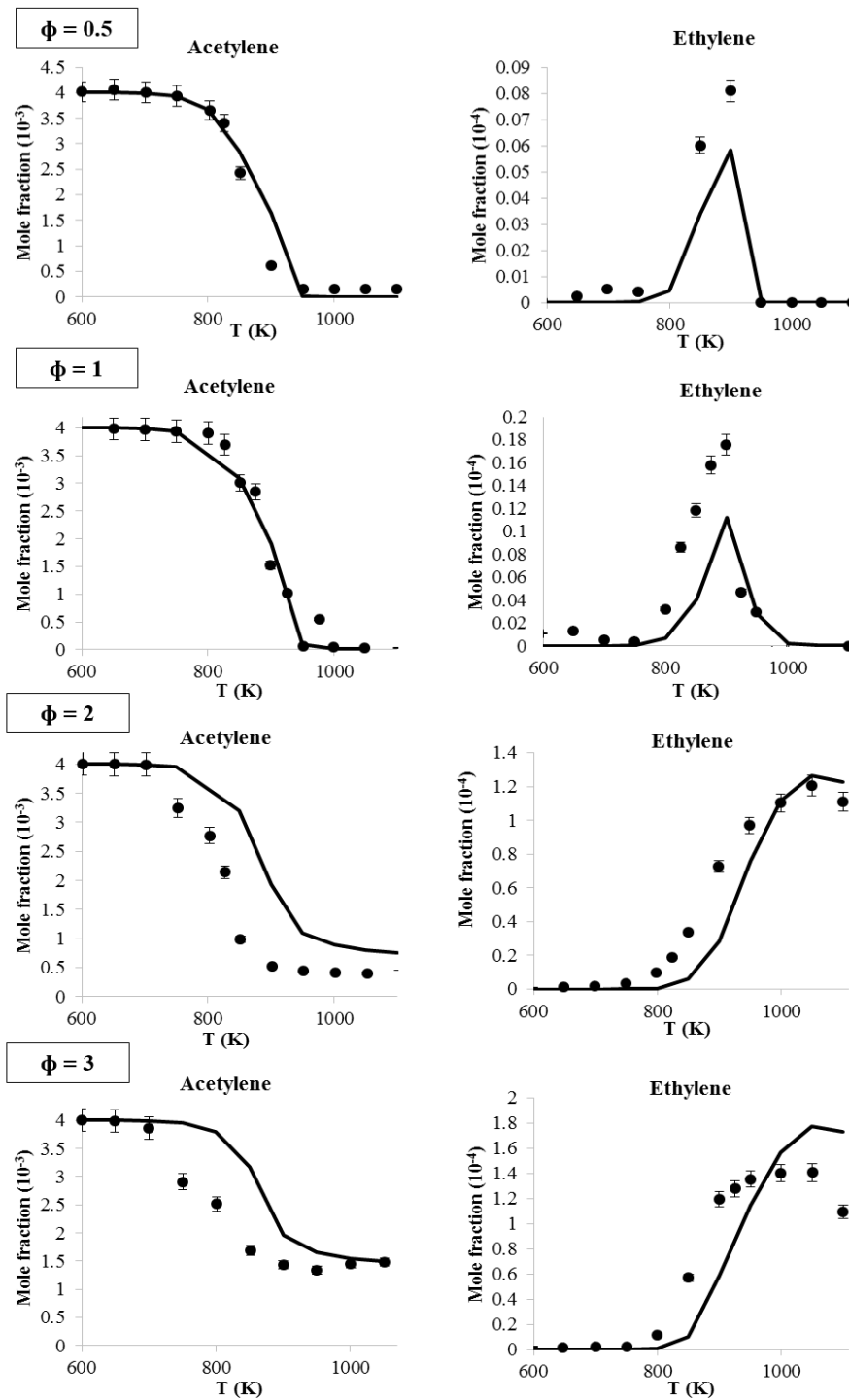


Fig.14. Equivalence ratio (ϕ) effect on acetylene oxidation: Comparisons between model predictions (lines) and experimental data (points) [85]. Error bars correspond to an uncertainty of 5% as given by the authors.

Benzene oxidation was conducted in a tubular reactor by Alzueta *et al.* [84] using different operating conditions (residence time, temperature, inlet composition). It is overall satisfyingly

predicted by the BioPOx model. On the same way, experiments performed by Zhang *et al.* [82] on the pyrolysis of toluene in a tubular reactor are well predicted by the the BioPOx model.

As a last example of those compounds, ethylbenzene pyrolysis was conducted in a tubular reactor by Yuan *et al.* [86]. For the different studied pressures, as is shown in Fig. 15, model predictions are in a good agreement with experimental results for ethylbenzene degradation and benzene formation.

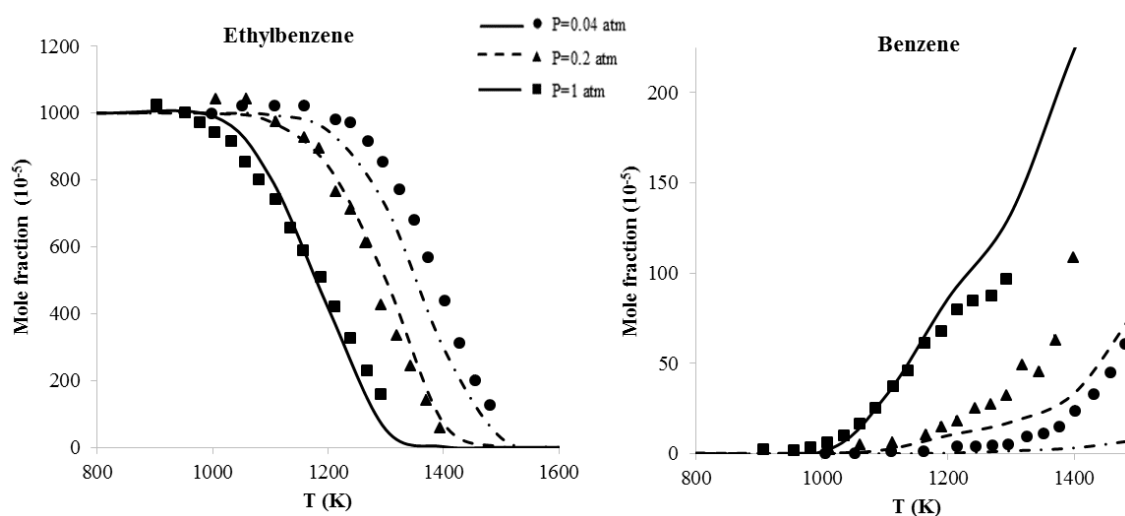


Fig.15. Pressure effect on ethylbenzene pyrolysis: Comparisons between model predictions (lines) and experimental data (points) [86], Error bars correspond to an uncertainty of 25% as given by the authors.

The BioPox model has also been validated on three pyrolysis and oxidation studies of wood and its components, in particular, in the work of Thimthong *et al.* [78]. These authors carried out the pyrolysis of cedar wood, as well as the partial oxidation of the produced volatile compounds for two different temperatures (700 °C and 800 °C) in a two-stage tubular reactor. This reactor was modeled using a network of reactors connecting a PSR for pyrolysis to a PFR for oxidation, using for the CHEMKIN-PRO simulation the flowsheet shown in the spreadsheet in Supplementary Material. Fig.16. shows major gases (CO, CO₂, H₂ and CH₄) yields as a

function of the residence time at 800 °C. Overall, an acceptable agreement is found between model predictions and experimental results.

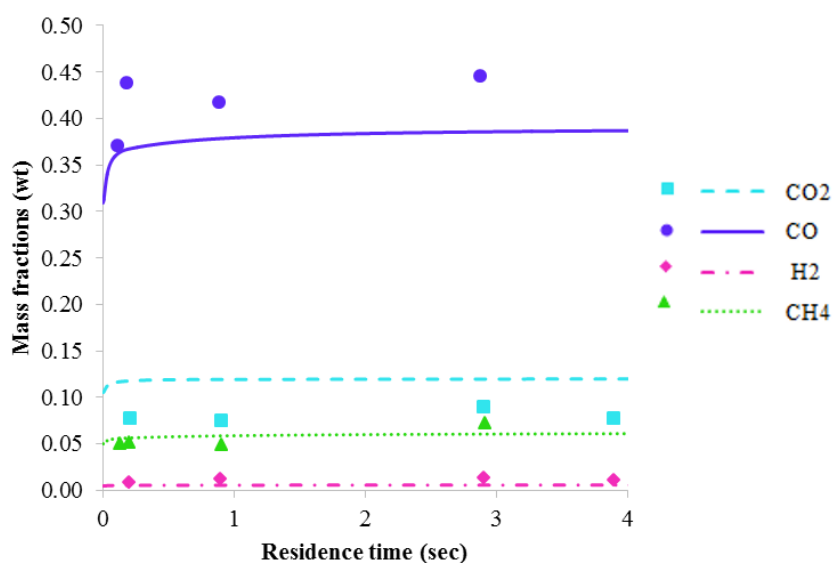


Fig.16. Major gases (CO, CO₂, H₂ and CH₄) yields as a function of the residence time during the pyrolysis of cedar wood and the partial oxidation of the volatile compounds: Comparisons between model predictions (lines) and experimental data (points) [85].

The pyrolysis of cellulose has been also studied with the BioPOx model, in particular, on the work of Norinaga *et al.* [80]. They studied the pyrolysis of pure cellulose for three different temperatures 700 °C, 750 °C and 800 °C in a two-stage tubular reactor. Comparison between experimental results and model predictions for major gases and benzene yields as a function of the residence time is shown in Fig.17.

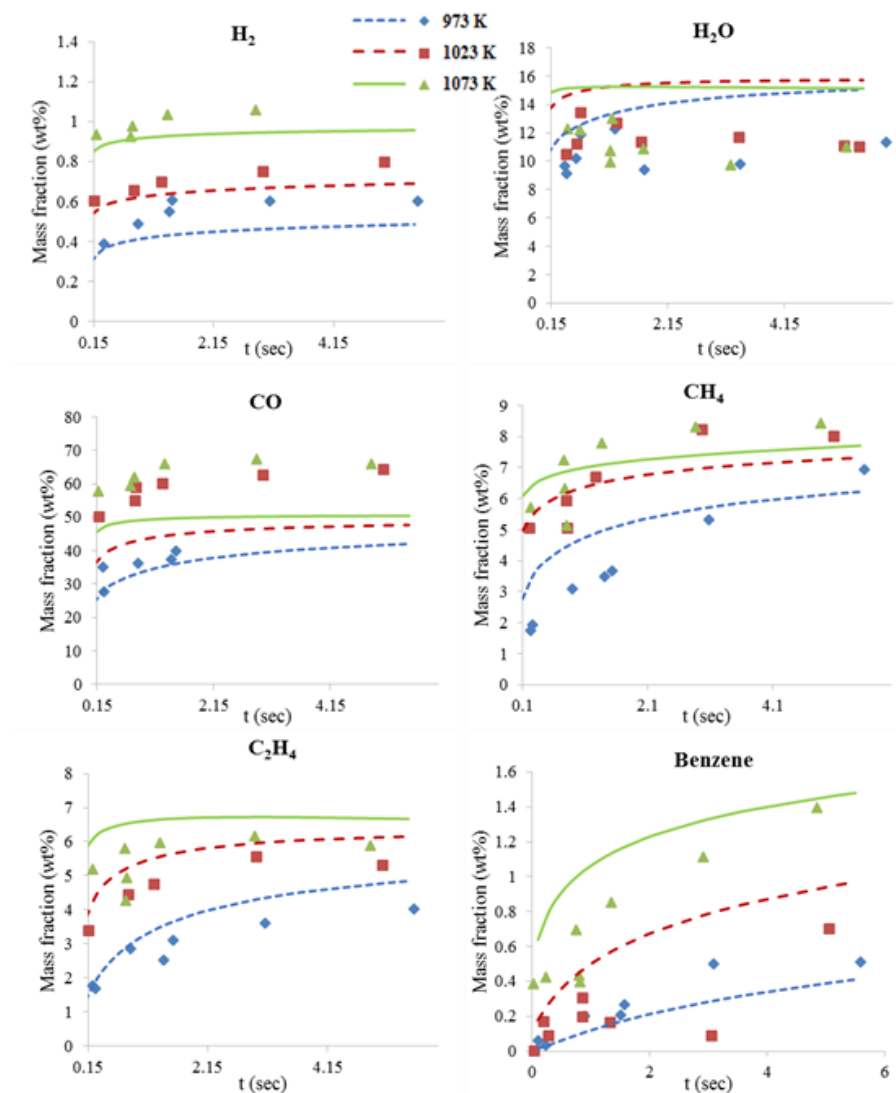


Fig.17. Major gases (CO, H₂O, H₂, CH₄ and C₂H₄) and benzene yields as a function of the residence time during the pyrolysis of cellulose: Comparisons between model predictions (lines) and experimental data (points)[80].

Conclusion

In the present work, we have developed a new kinetic model of wood combustion. To the best of our knowledge, this is the most detailed mechanism for biomass degradation since it considers in details the gas-phase reactions of the tars produced by the biomass devolatilization. Contrary to the existing lumped kinetic models, our model involves 710 species and includes

5035 reactions, amongst which 5006 gas-phase elementary reactions. This paper shows that BioPOx (Biomass Pyrolysis and Oxidation) model can predict results obtained for a wide range of experimental devices (tubular, jet stirred reactor, fluidized bed, closed ampoule...) and operating conditions (temperatures from 100 °C to 1327 °C, equivalence ratios from 0.5 to 3 and pressures from 4 kPa to 106.7 kPa).

The first part of BioPOx model consists in a semi-detailed mechanism from the literature used to describe biomass pyrolysis. This devolatilization mechanism was newly tested against TGA results obtained in parallel of this work, and against a set of 10 data from the literature. These comparisons show that the model is able to reproduce experimental results of TGA for wood and its constituents, under inert or oxidative atmosphere at low to moderate heating rates. In future works, this pyrolysis mechanism should be improved to better reproduce results with high heating rates.

Gas-phase reactions induced by the combustion of volatile species produced by the biomass devolatilization are considered in the second part of the BioPOx model. A new detailed kinetic oxidation mechanism was proposed for hydroxyacetaldehyde which is one of the most important products derived from the pyrolysis of holocellulose (cellulose-hemicellulose association).

The new BioPOx model was validated against experimental results for pyrolysis and combustion of biomass, key compounds of biomass pyrolysis, and key compounds for PAH formation (a set of 19 data from the literature). These comparisons show that, as a whole, the model predictions, match reasonably well with experimental data. Note however that, for better validate this model, more studies on a wider range of tars would be needed with especially a more comprehensive analysis of combustion products. For high temperatures and large biomass particles, physical phenomena such as heat and mass transfer cannot be neglected. To predict pollutant emissions from domestic wood combustion appliances, the kinetic model BioPOx

should be coupled to a thermal model which will be the purpose of a second paper. Note however than before being of use in CFD modelling, the present kinetic model, which includes 710 species and 5035 reactions should be significantly reduced.

Acknowledgment

The authors gratefully acknowledges the Agence De l'Environnement et de la Maitrise de l'Energie (ADEME) for the financial support of this work, as well as the team of Prof. E. Ranzi for providing help for first using their biomass pyrolysis mechanism.

Supplementary data

Supplementary data associated with this article can be found, in the on line version:

- Detailed kinetic mechanism in format Chemkin: BioPOx meca.txt
- Thermodynamic data for involved species: BioPOx thermo.txt
- Spreadsheet of the tests of the devolatilization mechanism against experimental studies from literature: Tests of the devolatilization mechanism.xlsx
- Spreadsheet of the tests of BioPOx model against experimental studies from literature: Tests of BioPOx model.xlsx

References

- [1] World Meteorological Organization. WMO Greenhouse Gas Bulletin. WMO Bull 2017:1–8. doi:ISSN 2078-0796.
- [2] Haberle I, Skreiberg Ø, Łazar J, Haugen NEL. Numerical models for thermochemical degradation of thermally thick woody biomass, and their application in domestic wood heating appliances and grate furnaces. *Prog Energy Combust Sci* 2017;63:204–52. doi:10.1016/j.pecs.2017.07.004.
- [3] World Health Organization. Residential heating with wood and coal: health impacts and policy options in Europe and North America 2015:58.
- [4] Mettler MS, Vlachos DG, Dauenhauer PJ. Top ten fundamental challenges of biomass pyrolysis for biofuels. *Energy Environ Sci* 2012;5:7797–809. doi:10.1039/C2EE21679E.
- [5] Liu WJ, Li WW, Jiang H, Yu HQ. Fates of Chemical Elements in Biomass during Its Pyrolysis. *Chem Rev* 2017;117:6367–98. doi:10.1021/acs.chemrev.6b00647.
- [6] Popova E, Chernov A, Maryandyshev P, Alain B, Kehrli D, Trouv G, et al. Thermal degradation and combustion of wood fuels, coals and hydrolyzed lignin from the Russian Federation: experiments and modeling. *Bioresour Technol* 2016.
- [7] Zhou Z, Jin H, Zhao L, Wang Y, Wen W, Yang J, et al. A thermal decomposition study of pine wood under ambient pressure using thermogravimetry combined with synchrotron vacuum ultraviolet photoionization mass spectrometry. *Proc Combust Inst* 2017;36:2217–24. doi:10.1016/j.proci.2016.06.081.
- [8] Papari S, Hawboldt K. A review on the pyrolysis of woody biomass to bio-oil: Focus on

- kinetic models. *Renew Sustain Energy Rev* 2015;52:1580–95. doi:10.1016/j.rser.2015.07.191.
- [9] Dhyani V, Bhaskar T. A comprehensive review on the pyrolysis of lignocellulosic biomass. *Renew Energy* 2018;129:695–716. doi:10.1016/j.renene.2017.04.035.
- [10] Kan T, Strezov V, Evans TJ. Lignocellulosic biomass pyrolysis: A review of product properties and effects of pyrolysis parameters. *Renew Sustain Energy Rev* 2016;57:126–1140. doi:10.1016/j.rser.2015.12.185.
- [11] Collard FX, Blin J. A review on pyrolysis of biomass constituents: Mechanisms and composition of the products obtained from the conversion of cellulose, hemicelluloses and lignin. *Renew Sustain Energy Rev* 2014;38:594–608. doi:10.1016/j.rser.2014.06.013.
- [12] Larfeldt J, Leckner B, Melaen MC. Modelling and measurements of heat transfer in charcoal from pyrolysis of large wood particles. *Biomass and Bioenergy* 2000;18:507–14. doi:10.1016/S0961-9534(00)00008-8.
- [13] Galgano A, Di Blasi C, Horvat A, Sinai Y. Experimental validation of a coupled solid- and gas-phase model for combustion and gasification of wood logs. *Energy and Fuels* 2006;20:2223–32. doi:10.1021/ef060042u.
- [14] Yuen RKK, Yeoh GH, De Vahl Davis G, Leonardi E. Modelling the pyrolysis of wet wood - I. Three-dimensional formulation and analysis. *Int J Heat Mass Transf* 2007;50:4371–86. doi:10.1016/j.ijheatmasstransfer.2007.01.008.
- [15] Yang Y., Sharifi VN, Swithenbank J, Ma L, Darvell LI, Jones JM, et al. Combustion of a Single Particle of Biomass. *Energy & Fuels* 2008;22:306–16. doi:10.1021/ef700305r.
- [16] Galgano A, Di Blasi C, Ritondale S, Todisco A. Numerical simulation of the glowing

- combustion of moist wood by means of a front-based model. *Fire Mater* 2014;639–58. doi:10.1002/fam.
- [17] Ding Y, Wang C, Lu S. Modeling the pyrolysis of wet wood using FireFOAM. *Energy Convers Manag* 2015;98:500–6. doi:10.1016/j.enconman.2015.03.106.
- [18] Grønli MG, Melaaen MC. Mathematical Model for Wood Pyrolysis Comparison of Experimental Measurements with Model Predictions. *Energy & Fuels* 2000;14:791–800. doi:10.1021/ef990176q.
- [19] Bryden KM, Hagge MJ. Modeling the combined impact of moisture and char shrinkage on the pyrolysis of a biomass particle. *Fuel* 2003;82:1633–44. doi:10.1016/S0016-2361(03)00108-X.
- [20] Sand U, Sandberg J, Larfeldt J, Bel Fdhila R. Numerical prediction of the transport and pyrolysis in the interior and surrounding of dry and wet wood log. *Appl Energy* 2008;85:1208–24. doi:10.1016/j.apenergy.2008.03.001.
- [21] Sadhukhan AK, Gupta P, Saha RK. Modelling and experimental studies on pyrolysis of biomass particles. *J Anal Appl Pyrolysis* 2008;81:183–92. doi:10.1016/j.jaap.2007.11.007.
- [22] Kwiatkowski K, Bajer K, Celińska A, Dudyński M, Korotko J, Sosnowska M. Pyrolysis and gasification of a thermally thick wood particle - Effect of fragmentation. *Fuel* 2014;132:125–34. doi:10.1016/j.fuel.2014.04.057.
- [23] Branca C, Di Blasi C. Global interinsic kinetics of wood oxidation. *Fuel* 2004;83:81–7. doi:10.1016/S0016-2361(03)00220-5.
- [24] González JF, Encinar JM, Canito JL, Sabio E, Chacón M. Pyrolysis of cherry stones: Energy uses of the different fractions and kinetic study. *J Anal Appl Pyrolysis*

- 2003;67:165–90. doi:10.1016/S0165-2370(02)00060-8.
- [25] Radmanesh R, Courbariaux Y, Chaouki J, Guy C. A unified lumped approach in kinetic modeling of biomass pyrolysis. *Fuel* 2006;85:1211–20. doi:10.1016/j.fuel.2005.11.021.
- [26] Barneto AG, Carmona JA, Alfonso JEM, Serrano RS. Simulation of the thermogravimetry analysis of three non-wood pulps. *Bioresour Technol* 2010;101:3220–9. doi:10.1016/j.biortech.2009.12.034.
- [27] Shafizadeh F, Bradbury A. GW. Thermal degradation of cellulose in air and nitrogen at low temperatures. *J Appl Polym Sci* 1979;23:1431–42. doi:10.1002/app.1979.070230513.
- [28] Ranzi E, Cuoci A, Faravelli T, Frassoldati A, Migliavacca G, Pierucci S, et al. Chemical kinetics of biomass pyrolysis. *Energy and Fuels* 2008;22:4292–300. doi:10.1021/ef800551t.
- [29] Debiagi PEA, Pecchi C, Gentile G, Frassoldati A, Cuoci A, Faravelli T, et al. Extractives Extend the Applicability of Multistep Kinetic Scheme of Biomass Pyrolysis. *Energy and Fuels* 2015;29:6544–55. doi:10.1021/acs.energyfuels.5b01753.
- [30] Dussan K, Dooley S, Monaghan R. Integrating compositional features in model compounds for a kinetic mechanism of hemicellulose pyrolysis. *Chem Eng J* 2017;328:943–61. doi:10.1016/j.cej.2017.07.089.
- [31] Dussan K, Dooley S, Monaghan RFD. A model of the chemical composition and pyrolysis kinetics of lignin. *Proc Combust Inst* 2018;000:1–8. doi:10.1016/j.proci.2018.05.149.
- [32] Broadbelt LJ, Pfaendtner J. Lexicography of kinetic modeling of complex reaction networks. *AIChE J* 2005;51:2112–21. doi:10.1002/aic.10599.

- [33] Vinu R, Broadbelt LJ. A mechanistic model of fast pyrolysis of glucose-based carbohydrates to predict bio-oil composition. *Energy Environ Sci* 2012;5:9808–26. doi:10.1039/C2EE22784C.
- [34] Zhou X, Nolte MW, Mayes HB, Shanks BH, Broadbelt LJ. Experimental and Mechanistic Modeling of Fast Pyrolysis of Neat Glucose-Based Carbohydrates. 1. Experiments and Development of a Detailed Mechanistic Model. *Ind Eng Chem Res* 2014;53:13274–89. doi:10.1021/ie502259w.
- [35] Zhou X, Li W, Mabon R, Broadbelt LJ. A mechanistic model of fast pyrolysis of hemicellulose. *Energy Environ Sci* 2018;11:1240–60. doi:10.1039/c7ee03208k.
- [36] Horton SR, Mohr RJ, Zhang Y, Petrocelli FP, Klein MT. Molecular-Level Kinetic Modeling of Biomass Gasification. *Energy & Fuels* 2016;30:1647–61. doi:10.1021/acs.energyfuels.5b01988.
- [37] Gil MV, Casal D, Pevida C, Pis JJ, Rubiera F. Thermal behaviour and kinetics of coal/biomass blends during co-combustion. *Bioresour Technol* 2010;101:5601–8. doi:10.1016/j.biortech.2010.02.008.
- [38] Shen DK, Gu S, Luo KH, Bridgwater AV, Fang MX. Kinetic study on thermal decomposition of woods in oxidative environment. *Fuel* 2009;88:1024–30. doi:10.1016/j.fuel.2008.10.034.
- [39] Pérez A, Martín-Lara MA, Gálvez-Pérez A, Calero M, Ronda A. Kinetic analysis of pyrolysis and combustion of the olive tree pruning by chemical fractionation. *Bioresour Technol* 2018;249:557–66. doi:10.1016/j.biortech.2017.10.045.
- [40] Wang G, Zhang J, Shao J, Ren S. Characterisation and model fitting kinetic analysis of coal/biomass co-combustion. *Thermochim Acta* 2014;591:68–74.

doi:10.1016/j.tca.2014.07.019.

- [41] Navarrete Cereijo G, Curto-Risso P, Bizzo WA. Simplified model and simulation of biomass particle suspension combustion in one-dimensional flow applied to bagasse boilers. *Biomass and Bioenergy* 2017;99:38–48. doi:10.1016/j.biombioe.2017.01.030.
- [42] Mätzing H, Gehrman HJ, Seifert H, Stapf D. Modelling grate combustion of biomass and low rank fuels with CFD application. *Waste Manag* 2018;78:686–97. doi:10.1016/j.wasman.2018.05.008.
- [43] Ranzi E, Corbetta M, Manenti F, Pierucci S. Kinetic modeling of the thermal degradation and combustion of biomass. *Chem Eng Sci* 2014;110:2–12. doi:10.1016/j.ces.2013.08.014.
- [44] Corbetta M, Frassoldati A, Bennadji H, Smith K, Serapiglia MJ, Gauthier G, et al. Pyrolysis of Centimeter-Scale Woody Biomass Particles: Kinetic Modeling and Experimental Validation. *Energy & Fuels* 2014;28:1–6.
- [45] Debiagi PEA, Gentile G, Pelucchi M, Frassoldati A, Cuoci A, Faravelli T, et al. Detailed kinetic mechanism of gas-phase reactions of volatiles released from biomass pyrolysis. *Biomass and Bioenergy* 2016;93:60–71. doi:10.1016/j.biombioe.2016.06.015.
- [46] Ranzi E, Debiagi PEA, Frassoldati A. Mathematical Modeling of Fast Biomass Pyrolysis and Bio-Oil Formation. Note I: Kinetic Mechanism of Biomass Pyrolysis. *ACS Sustain Chem Eng* 2017;5:2867–81. doi:10.1021/acssuschemeng.6b03096.
- [47] Vassilev SV, Baxter D, Andersen LK, Vassileva CG. An overview of the chemical composition of biomass. *Fuel* 2010;89:913–33. doi:10.1016/j.fuel.2009.10.022.
- [48] Dorado J, Van Beek TA, Claassen FW, Sierra-Alvarez R. Degradation of lipophilic wood extractive constituents in *Pinus sylvestris* by the white-rot fungi *Bjerkandera* sp. and

- Trametes versicolor. Wood Sci Technol 2001;35:117–25. doi:10.1007/s002260000077.
- [49] Sharma A, Pareek V, Zhang D. Biomass pyrolysis - A review of modelling, process parameters and catalytic studies. Renew Sustain Energy Rev 2015;50:1081–96. doi:10.1016/j.rser.2015.04.193.
- [50] Ranzi E, Pierucci S, Aliprandi PC, Stringa S. Comprehensive and detailed kinetic model of a traveling grate combustor of biomass. Energy and Fuels 2011;25:4195–205. doi:10.1021/ef200902v.
- [51] Schmidt G, Trouvé G, Leyssens G, Schönnenbeck C, Genevray P, Cazier F, et al. Wood washing: Influence on gaseous and particulate emissions during wood combustion in a domestic pellet stove. Fuel Process Technol 2018;174:104–17. doi:10.1016/j.fuproc.2018.02.020.
- [52] Faravelli T, Frassoldati A, Migliavacca G, Ranzi E. Detailed kinetic modeling of the thermal degradation of lignins. Biomass and Bioenergy 2010;34:290–301. doi:10.1016/j.biombioe.2009.10.018.
- [53] ANSYS CHEMKIN 17.0 (15151), ANSYS Reaction Design: San Diego, 2016. n.d.
- [54] Williams PT, Besler S. The influence of temperature and heating rate on the slow pyrolysis of biomass 1996;1481:6–7.
- [55] Jakab E, Faix O, Till F, Szekely T. Thermogravimetry / mass spectrometry within the scope of an international study of six lignins round robin test. Anal Appl Pyrolysis 1995;35.
- [56] Shen D, Hu J, Xiao R, Zhang H, Li S, Gu S. Online evolved gas analysis by Thermogravimetric-Mass Spectroscopy for thermal decomposition of biomass and its components under different atmospheres: Part I . Lignin. Bioresour Technol

- 2013;130:449–56. doi:10.1016/j.biortech.2012.11.081.
- [57] Shen D, Ye J, Xiao R, Zhang H. TG-MS analysis for thermal decomposition of cellulose under different atmospheres. *Carbohydr Polym* 2013;98:514–21. doi:10.1016/j.carbpol.2013.06.031.
- [58] Werner K, Pommer L, Broström M. Thermal decomposition of hemicelluloses. *J Anal Appl Pyrolysis* 2014;110:130–7. doi:10.1016/j.jaap.2014.08.013.
- [59] Shen D, Zhang L, Xue J, Guan S, Liu Q, Xiao R. Thermal degradation of xylan-based hemicellulose under oxidative atmosphere. *Carbohydr Polym* 2015;127:363–71. doi:10.1016/j.carbpol.2015.03.067.
- [60] Le Brech Y, Jia L, Cissé S, Mauviel G, Brosse N, Dufour A. Mechanisms of biomass pyrolysis studied by combining a fixed bed reactor with advanced gas analysis. *J Anal Appl Pyrolysis* 2016;117:334–46.
- [61] Le Brech Y, Raya J, Delmotte L, Brosse N, Gadiou R, Dufour A. Characterization of biomass char formation investigated by advanced solid state NMR. *Carbon N Y* 2016;108:165–77. doi:10.1016/j.carbon.2016.06.033.
- [62] Chen D, Li Y, Cen K, Luo M, Li H, Lu B. Pyrolysis polygeneration of poplar wood : Effect of heating rate and pyrolysis temperature. *Bioresour Technol* 2016;218:780–8. doi:10.1016/j.biortech.2016.07.049.
- [63] Husson B, Ferrari M, Herbinet O, Ahmed SS, Glaude PA, Battin-Leclerc F. New experimental evidence and modeling study of the ethylbenzene oxidation. *Proc. Combust. Inst.*, vol. 34, 2013, p. 325–33. doi:10.1016/j.proci.2012.06.002.
- [64] Song Y, Marrodán L, Vin N, Herbinet O, Assaf E, Fittschen C, et al. The sensitizing effects of NO₂ and NO on methane low temperature oxidation in a jet stirred reactor.

- Proc Combust Inst 2018;000:1–9. doi:10.1016/j.proci.2018.06.115.
- [65] Battin-Leclerc F, Konnov AA, Jaffrezo JL, Legrand M. To better understand the formation of short-chain acids in combustion systems. *Combust Sci Technol* 2008;180:343–70. doi:10.1080/00102200701740782.
- [66] Tran LS, Wang Z, Carstensen HH, Hemken C, Battin-leclerc F, Kohse-höinghaus K. Comparative experimental and modeling study of the low- to moderate-temperature oxidation chemistry of 2, 5-dimethylfuran, 2-methylfuran, and furan. *Combust Flame* 2017;181:251–69. doi:10.1016/j.combustflame.2017.03.030.
- [67] Nowakowska M. Conversion thermique des goudrons provenant de la gazéification de la biomasse. Université de Lorraine, 2014.
- [68] Nowakowska M, Herbinet O, Dufour A, Glaude PA. Detailed kinetic study of anisole pyrolysis and oxidation to understand tar formation during biomass combustion and gasification. *Combust Flame* 2014;161:1474–88. doi:10.1016/j.combustflame.2013.11.024.
- [69] Nowakowska M, Herbinet O, Dufour A, Glaude PA. Kinetic Study of the Pyrolysis and Oxidation of Guaiacol. *J Phys Chem A* 2018:acs.jpca.8b06301. doi:10.1021/acs.jpca.8b06301.
- [70] Muller C, Michel V, Scacchi G, Côme GM. THERGAS: a computer program for the evaluation of thermochemical data of molecules and free radicals in the gas phase. *J Chim Phys* 1995;5:1154–78.
- [71] Baulch DL, Pilling MJ, Cobos CJ, Cox RA, Frank P, Hayman G, et al. Evaluated Kinetic Data for Combustion Modeling. Supplement I. *J Phys Chem Ref Data* 1994;23:847–8. doi:10.1063/1.555953.

- [72] Yasunaga K, Kubo S, Hoshikawa H, Kamesawa T, Hidaka Y. Shock-Tube and Modeling Study of Acetaldehyde Pyrolysis and Oxidation. *Int J Chem Kinet* 2008;40:73–102. doi:10.1002/kin.20294.
- [73] Allara DL, Shaw R. A compilation of kinetic parameters for the thermal degradation of n-alkane molecules. *J Phys Chem Ref Data* 1980;9:523–59.
- [74] Bloch-Michel V. KINGAS: software for the estimation of kinetic data based on Benson's method. Ph.D. thesis, Institut National Polytechnique de Lorraine, Nancy, 1995.
- [75] Tran LS, Glaude PA, Battin-Leclerc F. An experimental study of the structure of laminar premixed flames of ethanol/methane/oxygen/argon. *Combust Explos Shock Waves* 2013;49:11–8. doi:10.1134/S0010508213010024.
- [76] Shin EJ, Nimlos MR, Evans RJ. Kinetic analysis of the gas-phase pyrolysis of carbohydrates. *Fuel* 2001;80:1697–709. doi:http://dx.doi.org/10.1016/S0016-2361(01)00056-4.
- [77] Fukutome A, Kawamoto H, Saka S. Processes forming Gas, Tar, and Coke in Cellulose Gasification from Gas-Phase Reactions of Levoglucosan as Intermediate. *ChemSusChem* 2015;8:2240–9. doi:10.1002/cssc.201500275.
- [78] Thimthong N, Appari S, Tanaka R, Iwanaga K, Kudo S, Hayashi J, et al. Kinetic modeling of non-catalytic partial oxidation of nascent volatiles derived from fast pyrolysis of woody biomass with detailed chemistry. *Fuel Process Technol* 2015;134:159–67. doi:10.1016/j.fuproc.2015.01.029.
- [79] Hoekstra E, Westerhof RJM, Brilman W, Swaaij WPMV, Kersten SRA, Hogendoorn KJA, et al. Heterogeneous and Homogeneous Reactions of Pyrolysis Vapors from Pine Wood. *Wiley Online Libr* 2012;58. doi:10.1002/aic.

- [80] Norinaga K, Shoji T, Kudo S, Hayashi J. Detailed chemical kinetic modelling of vapour-phase cracking of multi-component molecular mixtures derived from the fast pyrolysis of cellulose. *Fuel* 2013;103:141–50. doi:10.1016/j.fuel.2011.07.045.
- [81] Cheng Z, Tan Y, Wei L, Xing L, Yang J, Zhang L, et al. Experimental and kinetic modeling studies of furan pyrolysis : Fuel decomposition and aromatic ring formation. *Fuel* 2017;206:239–47. doi:10.1016/j.fuel.2017.05.090.
- [82] Zhang R, Zhao S, Luo Y. Experimental and Modeling Investigation on the Effect of Intrinsic and Extrinsic Oxygen on Biomass Tar Decomposition. *Energy & Fuels* 2017;31:8665–73. doi:10.1021/acs.energyfuels.7b00989.
- [83] Asmadi M, Kawamoto H, Saka S. Thermal reactions of guaiacol and syringol as lignin model aromatic nuclei. *J Anal Appl Pyrolysis* 2011;92:88–98. doi:10.1016/j.jaap.2011.04.011.
- [84] Alzueta MU, Glarborg P, Dam-johansen K. Experimental and Kinetic Modeling Study of the Oxidation of Benzene. *Int J Chem Kinet* 2000;32:498–522.
- [85] Wang B, Liu Y, Weng J, Glarborg P. New insights in the low-temperature oxidation of acetylene. *Proc Combust Inst* 2017;36:355–63. doi:10.1016/j.proci.2016.06.163.
- [86] Yuan W, Li Y, Pengloan G, Togbé C, Dagaut P, Qi F. A comprehensive experimental and kinetic modeling study of ethylbenzene combustion 2016;166:255–65. doi:10.1016/j.combustflame.2016.01.026.
- [87] Saggese C, Frassoldati A, Cuoci A, Faravelli T, Ranzi E. A wide range kinetic modeling study of pyrolysis and oxidation of benzene. *Combust Flame* 2013;160:1168–90. doi:10.1016/j.combustflame.2013.02.013.